The Journal of Engineering

WILEY

IET The Institution of Engineering and Technology

ORIGINAL RESEARCH OPEN ACCESS

Cost-Effective Optimal Integration of Renewable Energy and Waste-to-Energy Technologies

Md Sajjad-Ul Islam[1] | Md. Arafat Bin Zafar[1] | Md. Rashidul Islam[2] | Arafat Ibne Ikram[3] | Md Shafiullah[4,5]

[1]Department of Electrical and Electronic Engineering, Friedrich-Alexander-Universität Erlangen-Nürnberg (FAU), Erlangen, Germany | [2]Department of Electrical and Electronic Engineering, Noakhali Science and Technology University, Noakhali, Bangladesh | [3]Department of Electrical and Electronic Engineering, International Islamic University Chittagong, Chattogram, Bangladesh | [4]Control & Instrumentation Engineering Department, King Fahd University of Petroleum & Minerals, Dhahran, Saudi Arabia | [5]Interdisciplinary Research Center for Sustainable Energy Systems, King Fahd University of Petroleum & Minerals, Dhahran, Saudi Arabia

Correspondence: Md. Rashidul Islam (rashidul.cuet@gmail.com) | Arafat Ibne Ikram (arafatibne.ikram@gmail.com) | Md Shafiullah (shafiullah@kfupm.edu.sa)

Received: 8 December 2024 | **Revised:** 13 September 2025 | **Accepted:** 21 November 2025

ABSTRACT

The growing demand for reliable and clean energy in remote regions necessitates innovative solutions that balance economic viability and sustainability. This study proposes a novel cost-effective optimization framework for a hybrid microgrid integrating photovoltaic (PV) panels, wind turbines (WT), waste-to-energy (WtE) systems based on FastOx gasification, diesel generators (DG), and battery energy storage. The primary objective is to minimize the levelized cost of energy (LCoE) and greenhouse gas emissions while ensuring energy reliability. A hybrid optimization approach utilizing particle swarm optimization (PSO) and grey wolf optimization (GWO) is developed to determine the optimal sizing of system components. The methodology is applied to a real-world case study in Halishahar, Bangladesh, incorporating local meteorological data and municipal solid waste profiles. Simulation results show that GWO achieves the lowest LCoE of 0.221 $/kWh, outperforming PSO (0.223 $/kWh) and HOMER software (0.468 $/kWh). Additionally, the integration of WtE reduces emissions and enhances energy diversity. Comparative analyses validate the convergence and effectiveness of the proposed method, demonstrating its superiority in terms of techno-economic and environmental performance compared to existing approaches. This research provides a practical pathway for the sustainable deployment of microgrids in developing countries.

1 | Introduction

Global electricity demand is steadily rising due to the development and modernization of countries worldwide. Such a rise in demand comes with a challenge in terms of ensuring a consistent and sustainable energy supply. Although fossil fuel-based electricity production is easily accessible, it has considerable environmental consequences and contributes to climate change. In response, renewable energy sources (RES) are gaining popularity as the world requires additional energy and seeks a sustainable and diverse range of energy options [1–3]. A hybrid renewable energy system (HRES) is a combination of various power generation capacities that utilize renewable resources, such as solar, wind, biomass, and hydrogen fuel, as well as generators powered by fossil fuels, to meet demand. The intermittent nature of the dominant RE sources, for example, solar and wind, is a crucial issue for consideration before large-scale deployment [4–7]. Microgrids, small power systems comprising various combinations of generation, storage systems, and loads that can be operated independently or through integration with main utility grids, are suggested as a possible solution to the climate change problem through the utilization of renewable resources. The small-scale grids utilize renewable energy sources, making the electricity supply reliable and efficient for customers.

In literature, several advanced strategies have been proposed for microgrid sizing and the efficient management of their energy to make them economical and environmentally sustainable [8–10]. Microgrids can be an excellent option for the citizens of developing countries like Bangladesh [11], as many people in rural areas and remote islands still don't have access to a reliable flow of electrical energy through the national grid. To deal with the emissions of carbon dioxide (CO_2) and other gases, researchers suggested the utilization of WtE based renewable resources along with other available resources for the electrification of the remote and rural areas of developing countries.

Recent literature presents a diverse range of optimization approaches and modeling tools for hybrid energy systems. For instance, one study utilized a Monte Carlo simulation coupled with a genetic algorithm to evaluate the uncertainty and optimization of hybrid systems [1]. Although this approach effectively quantifies risk and variability, it lacks practical deployment with real WtE integration or region-specific resource availability. Some studies have been conducted on the optimization of component parameters and the management of energy in hybrid renewable systems, including optimal sizing of a hybrid microgrid based on typical scenarios considering meteorological variability [12], a microgrid comprising of solar PV, diesel generator, wind turbine, and battery bank system is tested against different weather conditions for the location IRAN [13], a multi-objective optimization of PV, wind, biomass and battery-based grid-integrated hybrid renewable energy system [14], energy management system for a grid-connected microgrid with PV and battery [15, 16], a multi-objective energy management optimization for grid-connected microgrids [17] and energy management for on-grid and off-grid wind/PV and battery hybrid systems [18].

Table 1 shows the major findings and research gaps of some previous works discussed above.

A few studies have incorporated waste into hybrid systems. One study that proposed a waste-incorporated microgrid was for pyrolysis and anaerobic gasification for different waste types [21], while a distinct study was focused on identifying the most effective algorithm for minimizing the total net present cost of the system [22]. While alternative green technologies are being explored–such as hydrogen production from PV and hybrid energy systems [23]–they often demand high infrastructure investment and rigorous safety protocols. Conversely, WtE solutions present a more regionally scalable and immediate deployment opportunity [24, 25]. Financial and technical tools have also been developed to aid in system sizing and economic analysis. For example, reference [26] offers a tool for sizing and cost analysis of battery systems, but it does not incorporate waste utilization or consider environmental metrics like CO_2 emissions. A more holistic evaluation is achieved when technical sizing is combined with LCoE and emission minimization [27, 28]. Despite the substantial progress in hybrid energy system optimization, notable gaps remain:

- A lack of studies integrating WtE technologies with conventional renewable microgrids (PV, wind, battery) and energy management systems.
- Limited use of real-world datasets, especially in regions with varying meteorological and waste characteristics
- A scarcity of benchmarking using multiple optimization tools.

Few works focus on balancing energy, environmental, and economic performances simultaneously [27–31]. Furthermore, while some recent efforts have applied PSO-based optimization to enhance energy and environmental performance in WtE systems using gasification and solid oxide fuel cells [32], they do not address the broader integration of WtE with a hybrid RE-battery framework. Therefore, this study aims to bridge these gaps by integrating FastOx-based WtE technology with renewable energy components and storage systems, employing real meteorological and municipal solid waste data. A combination of metaheuristic optimization and hybrid optimization of multiple electric renewable (HOMER) simulation is used to ensure both computational rigor and practical feasibility, with a focus on minimizing LCoE and emissions, providing a comprehensive, scalable, and environmentally sound energy solution.

This study adopts a scenario-based approach to enhance WtE integrated microgrid systems, aiming to reduce both the LCoE and carbon emissions. Focusing specifically on the context of Bangladesh, the research explores Meta-heuristic optimization techniques alongside traditional and aftermarket HOMER-based solutions. Meta-heuristic algorithms emerge as effective tools for tackling the complexities inherent in optimizing hybrid renewable energy systems (HRES), even amidst vast and intricate search spaces. Furthermore, the research underscores the significance of economic feasibility and seeks validation through the utilization of HOMER software. This software serves as a valuable tool for implementing meta-heuristic algorithms in optimizing HRES design, boasting a user-friendly interface and facilitating intuitive specification of problem parameters. The major contributions of the article are as follows:

- Formulation of HRES for energy management problem considering regional renewable resources and load demand.
- Integration of the WtE and energy storage resources into the system while assessing capital expenditure and economic feasibility.
- Deployment of two meta-heuristic optimization algorithms alongside HOMER optimization to minimize LCoE and reduce emissions.

The remaining parts of this research are structured in the following manner. The microgrid mathematical form is shown in Section 2, and Section 3 lays out the plan for managing energy consumption. The objectives and objective functions are outlined in Section 4 and the optimization methods are discussed in Section 5. Section 6 discusses the selection of location, load demand data, and other input data. The effectiveness of the used algorithms is shown by a discussion of the results with the statistical analysis in Section 7, and the conclusion is given at the end in Section 8.

TABLE 1 | Summary of literature review.

References	Study	Major findings	Research gap
[15]	A PV-battery grid-integrated system based on cost minimization and maximization of the utilization of the sources.	The M-EMS includes forecasting for solar irradiance, temperature, and load demand, along with optimization for efficient power generation and load scheduling in a grid-connected microgrid.	Cost analysis and fluctuating renewable sources and loads are not considered.
[17]	A novel expert system fuzzy logic-grey Wolf Optimization (FL-GWO) based intelligent meta-heuristic method for battery sizing and energy management in grid-connected microgrids.	The proposed method outperforms existing approaches like GA, PSO, BA, IBA, and GWO in satisfying microgrid demands and minimizing operating costs, as demonstrated through simulations across various scenarios	Proper mathematical modeling of the sources is not considered in the system design.
[18]	A PV, wind, and battery-based grid-integrated system to power small loads.	A hybrid system control unit enables seamless operation on both grid and off-grid modes, boosting efficiency by up to 10%.	Did not consider cost optimization but only focused on energy transfer aspects
[19]	A novel metaheuristic method for maximizing the economic impact of grid participation on a microgrid system	A strategy combining whale optimization algorithm (WOA) and sine-cosine algorithm (SCA).	The method is computationally heavy and hasn't been tested on large microgrid systems.
[20]	A layout optimization of non-homogeneous wind farms.	Various optimization techniques are suggested for designing non-uniform wind farms efficiently.	It is computationally critical, as the formulation involves several variables and numerous constraints.

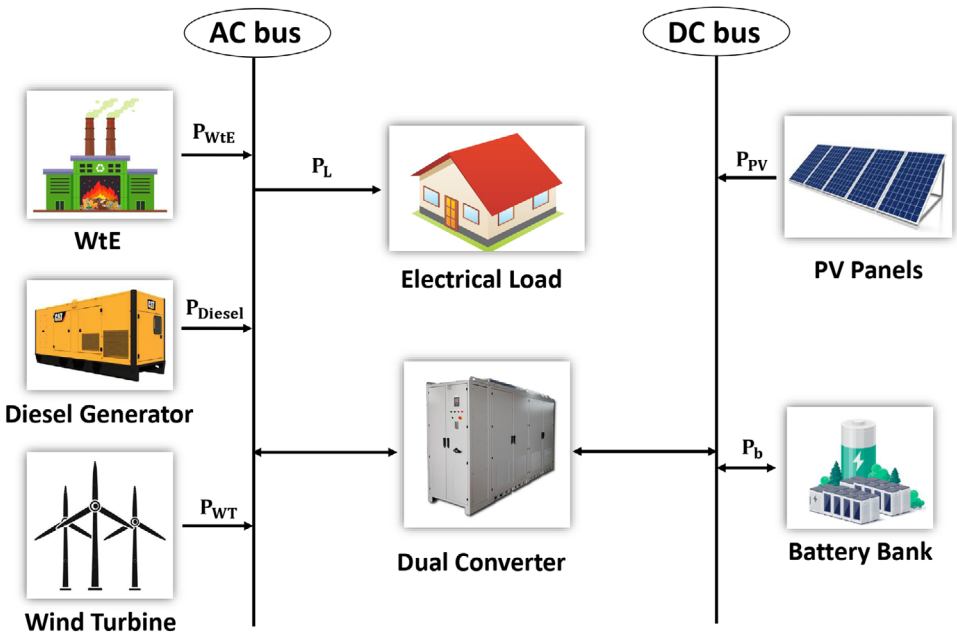

FIGURE 1 | Microgrid power generation system.

2 | Microgrid Model

The microgrid system depicted in Figure 1 comprises a solar PV farm, a wind farm, a WtE plant, a DG, a bank of batteries, and converters that allow voltage adjustments or conversion between alternating current (AC) and direct current (DC). On the DC side, a PV farm and a battery bank are connected, whereas, on the AC side, a wind farm, a WtE plant, and a DG are connected. Using the optimization model, it is possible to minimize the LCoE and greenhouse gas emissions. According to the information presented in Figure 1, the primary sources of RE are revealed to be WT and PV. To accomplish the goal of generating energy from

waste, the WtE system is put into operation. The load is connected directly to the distributed microgrid energy system. During periods of increased production, surplus energy can be stored in an energy storage system for later use. Conversely, during periods of decreased production, a DG can be employed as a backup. In this section, the mathematical interpretation and underlying function are explained for the microgrid system components.

2.1 | PV Model

Equation (1) is applied for the purpose of determining the power generated by a PV farm.

$$P_{pv}(t) = P_r^s \frac{G_h(t)}{G_S}[1 + k_t(0.0256G_h(t) + T_{amb}(t) - T_S)] \quad (1)$$

The equation involves several variables, namely P_r^s denotes the PV farm rating, $G_h(t)$ is the hourly solar radiation inclined at the tilted panel of the PV in units of (W/m^2), G_S denotes the standard incident radiation of 1000 W/m^2, k_t which takes a value of $-3.7 \times 10^{-3}(1/°C)$, $T_{amb}(t)$ denotes the hourly ambient temperature, and T_S represents the standard temperature of 25 $°C$ [33].

2.2 | WT Model

Equation (2) represents the model for determining the output power of a wind farm.

$$P_{wt}(t) = \begin{cases} 0 & V(t) \leqslant V_{cin} \text{ or } V(t) \geqslant V_{cout} \\ P_r^w & V_{rat} \leqslant V(t) \leqslant V_{cout} \\ P_r^w \left(\dfrac{V(t) - V_{cin}}{V_{rat} - V_{cin}} \right) & V_{cin} \leqslant V(t) \leqslant V_{rat} \end{cases} \quad (2)$$

The following formula depicts the power output of an individual wind turbine, where P_r^w represents the wind system rating, whereas V_{cin}, V_{cout}, V_{rat}, and $V(t)$ represent four distinct wind speeds, namely the cut-in speed, cut-out speed, rated wind speed, and wind speed at the target height, respectively [34]. There is a noticeable difference between the hub height and the reference height in terms of the average wind speed, which is a consequence of both site and location. It can be written as,

$$V(t) = V_r(t)\left(\frac{H_{WT}}{H_r} \right)^{\gamma} \quad (3)$$

In Equation (3), $V(t)$ is the wind speed at the hub height (H_{WT}), $V_r(t)$ is the wind speed at the reference height (H_r), and γ is the friction coefficient. For smooth surfaces at high exposure, the friction coefficient γ is typically 1/7 [35].

2.3 | WtE Model

Gasification technology is implemented to convert waste into useful energy. In general, it is a conversion method that transforms the chemicals that are left over after the recycling of waste into more valuable forms of energy, such as electricity. One study demonstrated that the WtE system, when combined with abundant solar and natural gas resources, single-objective optimization could enhance round-trip efficiency to 89.86%, and reduce the levelized cost of storage (LCOS) to $0.1873/kWh [27]. The WtE model is represented by the schematic diagram in Figure 2.

This model will make use of waste as a feedstock and combine it with oxygen, which is extracted from the air using a separation unit. This process is typically referred to as gasification using FastOx. As shown in Figure 2, garbage is introduced into the gasification process using the gasifier's top-mounted opening, and pure oxygen and steam flood in the center. The gasification reaction took place at temperatures of about 2,150°C [37]. As trash sinks to the gasifier's hottest section, it goes through a series of reaction stages. Particles of a distinct type are launched from each zone. Waste is converted into carbon char, inorganic materials, and metals in the gasifier's base layer. Using oxygen and steam, carbon char can be converted into synthesis gas, which is primarily made up of carbon monoxide and hydrogen. This reaction is highly exothermic, meaning it gives off a lot of heat energy. The waste accumulates at the bottom of the vessel and is heated by the gasifier as it interacts with the synthesis gas, reaching higher temperatures. At the top of the gasifier vessel, the synthetic gas is released and sent to the systems responsible for heat recovery and gas purification. Molten inorganic minerals and metals are collected at the gasifier's bottom. The determination of the high heating values (HHV) of the municipal solid waste (MSW) fraction is conducted through the utilization of a bomb calorimeter. Around 0.5-gram waste sample can be burned in an oxygen bomb at a pressure of roughly 2000 MPa [38]. Equation (4) demonstrates the comparatively modest thermal energy yield derived from the waste fractions utilized for the purpose of power generation.

$$LHV_{msw} = \sum_{1}^{9} W \times HV \quad (4)$$

The given equation involves the representation of LHV_{msw} as the low heating value, HV as the average heating value of MSW, and W as the percentage by weight. Equation (5) is employed to derive the energy potential recuperation from MSW, denoted as P_{WtE}.

$$P_{WtE} = LHV_{msw} \times W_{msw} \times \frac{1000}{3.6} \quad (5)$$

In this equation, P_{WtE} represents the energy potential from MSW, W_{msw} denotes the mass of MSW in units of tons, LHV_{msw} represents the net low heating value of the MSW (MJ/kg), and converting ratio (1 kWh = 3.6 MJ) [39].

2.4 | DG Model

The DG is essential to the system's dependability because it provides an electrical backup. For this reason, it is crucial to keep diesel production within a secure margin. Diesel production must be run within a typical operating range to prevent weakly loaded circumstances for efficient energy use and to achieve an acceptable safety margin for power fluctuations, such as a rapid rise in load consumption. While designing a microgrid, the fuel consumption of a DG can be mathematically represented by the

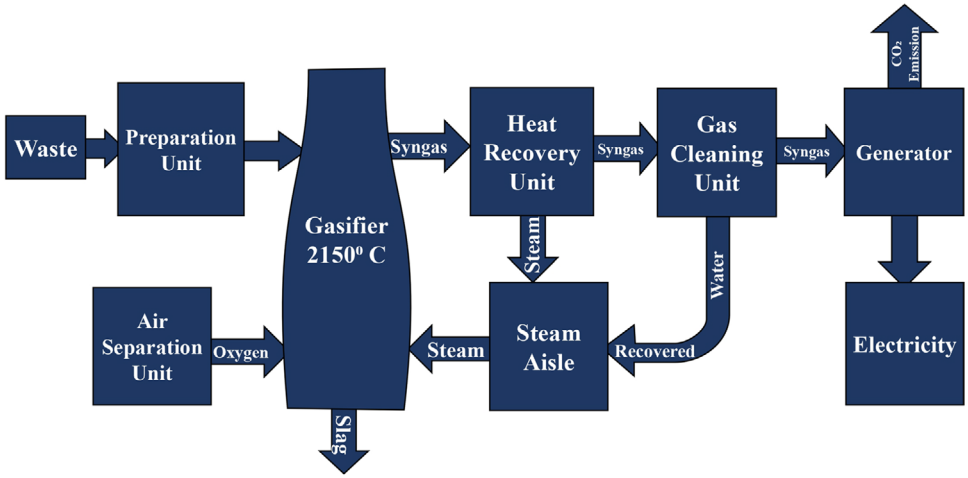

FIGURE 2 | Schematic diagram of WtE [36].

symbol $q(t)$.

$$q(t) = aP_{Diesel}(t) + bP_{rated} \tag{6}$$

Equation (6) represents the rated power as P_{rated}, the produced power as $P_{Diesel}(t)$, and the fuel consumption characteristics as a and b as coefficients. The values of a and b used in this analysis are 0.2461 and 0.08415, respectively [40].

2.5 | Battery Bank Model

Microgrids rely on batteries to store extra energy during times of abundant RE production and to provide electricity during hours of limited or no RE production. The assessment of the state of charge (SOC) is necessary in order to measure energy accurately. Equation (7) can be utilized to measure the battery SOC over a given duration.

$$\frac{SOC(t)}{SOC(t-1)} = \int_{T}^{T-1} \frac{P_b(t)\eta_{bat}}{V_{bus}} dt \tag{7}$$

The equation includes variables such as V_{bus}, $P_b(t)$, and η_{bat}, which, respectively, represent the bus voltage, input/output power of the battery, and the battery's round trip efficiency. When the value of $P_b(t)$ is positive, it indicates that the battery is undergoing a charging process. Conversely, if $P_b(t)$ is negative, it signifies that the battery is undergoing a discharging process [41]. A battery's round-trip efficiency can be described as,

$$\eta_{bat} = \sqrt{\eta_{bat}(ch) \times \eta_{bat}(dch)} \tag{8}$$

In Equation (8), the variables $\eta_{bat}(ch)$ and $\eta_{bat}(dch)$ represent the battery's efficiency when charging and discharging, respectively [42]. The battery bank is rated as having a 95% round-trip efficiency. The efficiency of charging is assumed to be 80%, whereas the efficiency of discharging is assumed to be 100%. The maximum SOC value is equal to the total capacity of the battery bank $C_n(Ah)$, and it is represented as follows:

$$C_n(Ah) = \frac{N_{bat}}{N_{bat}^S} C_b(Ah) \tag{9}$$

In Equation (9), $C_b(Ah)$ represents the capacity of a single battery, N_{bat} represents the number of batteries, and N_{bat}^S represents the number of batteries in series [42]. As the SOC_{min} of the battery bank is fixed, it cannot be discharged below that level. Parallel battery connections produce the required bus voltage. The number of batteries linked in series can be determined using the formula (10).

$$N_{bat}^S = \frac{V_{bus}}{V_{bat}} \tag{10}$$

Here, V_{bat} represents the voltage of a single battery in the circuit. The maximum charge or discharge power at any moment is also a crucial consideration in battery modeling. The following equation can be used to get the value based on the maximum charge current:

$$P_b^{max} = \frac{N_{bat} V_{bat} I_{max}}{1000} \tag{11}$$

In Equation (11), I_{max} in amperes represents the maximum charging current of the battery.

2.6 | Converter Model

Power conversion between DC and AC is required when a system also has DC components. It is necessary to convert DC power into AC to use which is generated by PV panels and batteries. The size of the converter is set by the peak load, denoted by $P_L^m(t)$ [43]. The power output of the converter, denoted by P_{inv}, may be calculated as follows:

$$P_{inv}(t) = P_L^m(t)/\eta_{inv} \tag{12}$$

In Equation (12), η_{inv} represents the efficiency of the converter.

2.7 | Greenhouse Gas Emission Estimation

Since there are no carbon emissions produced during the actual production of RE, the WtE plant and DG produced greenhouse

TABLE 2 | Emission factors.

Component name	GHG emission (kg CO_2 eq./kWh)
WtE plant	0.581 [44]
DG	1.092 [45]

gas (GHG). The GHG emissions ($kg\ CO_2\ eq.$) of power generation are estimated using Equation (13).

$$Emission_{total} = C_{wte} \sum_{1}^{8760} P_{wte} + C_{Diesel} \sum_{1}^{8760} P_{Diesel} \tag{13}$$

Here, C_{wte} and C_{Diesel} represent the CO_2 emission factor of WtE plant and DG, respectively. The carbon emission data by the WtE plant and DG is given on Table 2.

3 | Microgrid Energy Management Strategy (MEMS)

The deployment of MEMS must be a top priority during the system planning and development stages, as shown in Figure 3.

In this model, RES acted as the primary generator, so most of the energy was generated from the renewable source. The DG is used as a backup or dispatchable source, and the battery bank is charged when the system makes more electricity than it needs. If the power generated by renewable resources is more than what the load and battery bank need, the extra energy goes to a dump load. If the energy generated is less than what the load needs, the battery bank makes up the difference. When the RE source and the battery bank cannot meet the load requirements, the DG is turned on to meet the load requirements and charge the battery bank. Here, P_{WT} is energy generated from the wind turbine, $P_{PV}(t)$ is energy generated from the PV panel, $P_L(t)$ is the energy consumed by load demand at time t, η_{inv} is inverter efficiency, $P_{ch}(t)$ stands for the energy available for battery charging, $E_{ch}(t)$ indicates the energy charged to the battery, $P_{distch}(t)$ defines the energy that is to be discharged from battery, $E_{distch}(t)$ represents the energy discharged from battery, $E_{b_{max}}$ defines the maximum battery energy, $E_b(t)$ represents the energy of the battery, $E_{dump}(t)$ stands for the energy dumped (energy that can be used for an interruptible load like pumping load), *Diesel_hr(t)* define DG is running and *Diesel_power* is the power produced by a DG.

4 | Optimization Problem Formulation

The primary objective of this study is to design a microgrid system capable of fulfilling the energy demand at an affordable price and with minimal maintenance. Crucial factors include the power output and size of the PV panels, wind turbine, battery bank, and WtE. The primary objective of this research is to find the minimum net present cost (NPC) for the optimized system without sacrificing effectiveness. The number of components is the four primary decision elements chosen for the best configuration. In order to conduct a cost-benefit analysis, the annualized system cost (ASC) is employed. It is found that the solution with the lowest ASC also fulfills all other requirements. Total system cost, including capital cost, replacement cost, and operation and maintenance cost, is taken into account as the objective function. The capital costs of the components already include the prices of installation and labor costs. The following function is taken into account as the primary goal function that has to be reduced within the given restrictions.

$$ASC_{Minimize} = F(P_{pv}C_{pv} + N_{wt}C_{wt} + P_{wte}C_{wte} + N_{bat}C_{bat} + P_{inv}C_{inv}) \tag{14}$$

Equation (14) designates the costs of PV, WT, and inverters as C_{pv}, C_{wt}, and C_{inv}, respectively, in terms of per KW. Additionally, the cost of batteries is represented as C_{bat} per unit. The evaluation of WtE is represented by the variable P_{wte}, while the cost associated with WtE is represented by the variable C_{wte}. The symbol P_{inv} is used to represent the rating of the inverter [46].

The ASC of the installed component is comprised of a few different parts, including the installation cost C_{ai}, the annual maintenance cost C_{am}, the replacement cost C_{ar}, the operating cost C_f, and the salvage cost C_s. In addition to this, the total ASC of each component may be represented as follows:

$$C_{pv} = (C_{ai} + C_{am} + C_{ar} - C_s)_{pv} \tag{15}$$

$$C_{wt} = (C_{ai} + C_{am} + C_{ar} - C_s)_{wt} \tag{16}$$

$$C_{wte} = (C_{ai} + C_{am} + C_{ar} + C_f - C_s)_{wte} \tag{17}$$

$$C_{bat} = (C_{ai} + C_{am} + C_{ar} - C_s)_{bat} \tag{18}$$

$$C_{inv} = (C_{ai} + C_{am} + C_{ar} - C_s)_{inv} \tag{19}$$

It is possible to determine the yearly cost of any component with the assistance of a factor that is termed the capital recovery factor (CRF). The discount rate (i) used to compute the CRF is set at 6% aligning with typical energy project evaluation standards. The CRF is a tool for computing the worth of money at a particular point in time and can be given as:

$$CRF(i, N) = \frac{i(1+i)^N}{(1+i)^N - 1} \tag{20}$$

In Equation (20), the lifetime is represented in years as N, and the yearly interest rate is denoted by i [47]. By adhering to a set of boundaries, the objective of a function is reduced as much as possible, which may be summed up as:

$$1 \leqslant P_{pv} \leqslant P_{pv_m} \tag{21}$$

$$1 \leqslant N_{wt} \leqslant N_{wt_m} \tag{22}$$

$$1 \leqslant P_{wte} \leqslant P_{wte_m} \tag{23}$$

$$1 \leqslant N_{bat} \leqslant N_{bat_m} \tag{24}$$

$$SOC_{min} \leqslant SOC \leqslant SOC_{max} \tag{25}$$

The PV panel's maximum rating capacity is denoted by the value P_{pv_m}, the maximum units of batteries are denoted by N_{bat_m}, the

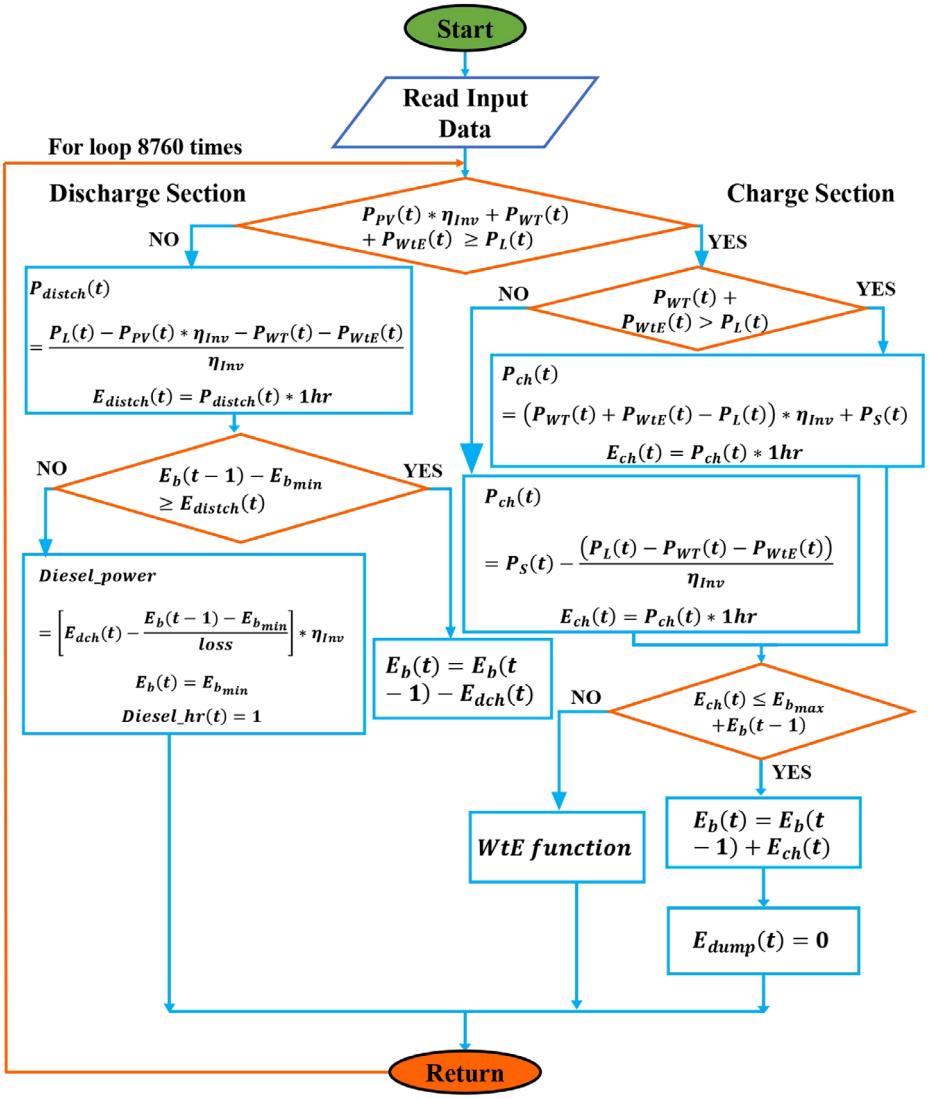

FIGURE 3 | Microgrid energy management strategy flowchart.

maximum units of WT is denoted by N_{wt_m}, and the maximum rating capacity of WtE is represented by P_{wte_m}.

The LCoE and highest dependability are taken into consideration while choosing the best configuration. It can be presented in Equation (26) [48].

$$LCoE = \frac{\text{ASC (\$/year)}}{\text{Total usable energy delivered (kWh/year)}} \quad (26)$$

Table 3 shows the per unit capacity, capital, replacement, operational & maintenance cost, and lifetime of all components individually that are used in the microgrid.

5 | Optimization Algorithms for Cost Minimization

Several studies have delved into the application of optimization algorithms in the design and energy management of microgrids. The utilization of HOMER software has proven instrumental in the design of microgrids, effectively mitigating costs and minimizing energy losses [51]. The PSO algorithm has found extensive application across diverse domains, including power grid planning, maintenance, and control [52]. Additionally, noteworthy advancements have been made in the GWO algorithm in recent years, facilitating its successful integration and application across various fields [53]. In this study, the optimization problem is formulated with a single objective: minimizing the net present cost (NPC) and associated LCoE of the microgrid system. Although the resulting GHG emissions are quantified and discussed, they are not explicitly minimized within the optimization model. The observed emissions are a byproduct of the optimized system configuration aimed solely at achieving cost-effectiveness. In this section, both the PSO and GWO methods are discussed. In addition to this, the HOMER optimization is carried out to validate and benchmark the outcomes of the algorithm and technique.

5.1 | HOMER Optimization

HOMER, an industry-standard program, employs a proprietary derivative-free algorithm in its Optimizer for estimating and

TABLE 3 | Price table of microgrid components [49, 50].

Components name	Per unit capacity	Capital cost	Replacement cost	Operation & maintenance cost	Lifetime in years
PV	1 kW	1500 ($)	—	0 ($/yr)	20
WT	kW	1300 ($)	1200 ($)	200 ($/yr)	20
WtE	1 kW	4000 ($)	—	150 ($/yr)	20
DG	1 kW	1200 ($)	1000 ($)	0.050 ($/yr)	10
Battery	7kWh				
(6V, 1156 Ah)	1250 ($)	1100 ($)	20 ($/yr)	10	
Converter	1 kW	800 ($)	750 ($)	20 ($/yr)	20
Discount rate (i)	6%				

optimizing microgrid systems, searching for the least-costly configuration [54]. Before installing a microgrid power system, the program is used to design it and determine its most efficient configuration in terms of stability, cost, size, and number of components. By only providing the information on location, load consumption, and component costs, as well as specifying the limits and dispatch strategy, it provides the economic structure of the examined system [55]. HOMER offers users a choice between two dispatch strategies: cycle charging and load following. In cycle charging, the generator runs at maximum capacity, using excess power to charge batteries. In load following, the generator starts and produces the exact amount of needed electricity.

5.2 | PSO

The algorithm depicted in Figure 4 is employed. MATLAB's Gaussian function is used to produce the random swarms of particle population. According to the initial restrictions of the PSO optimization, the value of these particles must be an integer. After that, the objective function is used to judge each population cluster individually. The procedure is designed to apply a significant penalty on the value that is determined to be optimum if any of the requirements are not satisfied. This allows the PSO to minimize the value of the goal function without risking a microgrid configuration that can't meet the load demand of the energy penetration scenario under consideration. The pseudocode and steps of the PSO are presented in "Appendix A". By carrying out these steps, it will be able to generate the best particle from the initial swarm of the population. Both the individual's top score and the overall highest score are recorded in separate variables. Following the completion of the program, the next iteration occurred. At this point, the software will verify the boundary to ensure that it does not exceed either the lowest or the maximum limit of the particle count. It will also update the weight and velocity of the particle. PSO is advantageous due to its fast early convergence, robustness in solving nonlinear and mixed-integer problems, and simple implementation with few control parameters [56]. Detailed information on PSO can be found in Ref. [57–59]

5.3 | GWO

The GWO's algorithmic flowchart is shown in Figure 5. The NPC of the MG is minimized using the GWO technique. Reduced operational costs for the system are the primary objective of the optimization. GWO can robustly maintain exploration and exploitation of optimal value faster than any other optimization technique. The pseudocode and steps of the GWO are presented in Appendix B. First, by using the MATLAB Gaussian function, a random sets of wolf populations are generated. The integer values of each wolf represent the capacity of the system. The best-fitted wolf will eventually be chosen for the outcome of the optimization. At first, every single wolf is evaluated using the objective function and classified into α, β, and γ. The best fitted among all wolves in the current generation is the α wolf. The second best fitted is the β, and the third best fitted is the class as γ. After that, each set of generations is tested for the microgrid system. If the sets of wolves can satisfy the optimization constraints, then it moves forward to the next iteration; otherwise, a big penalty is added to their fitness value so that they are already get rejected in the minimization process. Only the best-fitted wolf goes next iteration, and their position and the coefficient vector updated within them. Again the fitness is evaluated for the entire wolf and classified into α, β, and γ wolves. This fitness checking and position updating will go on until the iteration hits its maximum number or the termination criteria are met. By doing so, the optimal variable and the objective values are achieved. GWO offers a good balance between exploration and exploitation, faster convergence than PSO in complex nonlinear problems, and effectiveness in optimizing both discrete and continuous variables [56]. Detailed information on GWO can be found in references [60–62]

5.4 | Optimization Parameters

The program would have completed the specified number of iterations, or it would have satisfied the requirements for terminating the program. The essential parameters for PSO and GWO optimization are listed in Table 4, which can be found here.

6 | Analysis Condition

Regarding the case study, the economic feasibility of the suggested model was investigated by taking into account location-specific meteorological data, municipal solid waste, and electrical load demand.

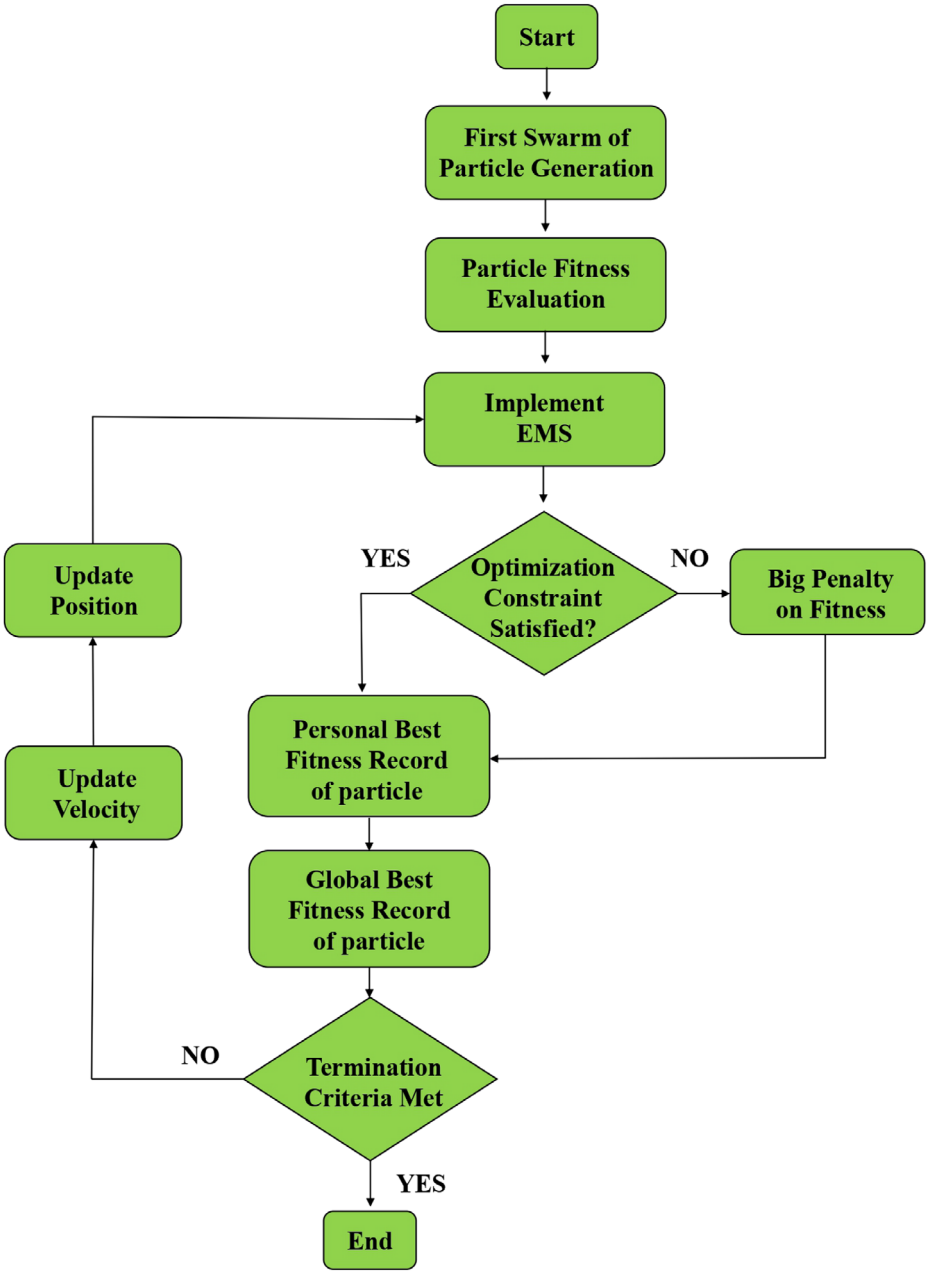

FIGURE 4 | PSO flowchart.

TABLE 4 | Optimization parameters for PSO and GWO.

Parameter	Value
Search agent	1024
Max iteration	500
Number of variables	4
Total run	3

6.1 | Site Selection

The Chattogram's Halishahar area is being considered for this microgrid power generation project because of its geographical location. Figure 6 depicts this area as having a size of 11.63 sq. km and is situated between the longitude of 91°45' - 91°48' south and latitude of 22°19' - 22°20' north [63].

The selected site has a wide variety of waste products as shown in Figure 7, where the top source of the waste is the household with the metric of 139 tons waste per day, proceeded by commercial waste having metric of 50 tons waste per day and last, street and construction waste ranked lowest with the metric of 39 tons waste per day [64], the waste stream comprises approximately 65% biodegradable materials and 35% non-biodegradable components. For modeling energy conversion, only the combustible fraction is used to estimate potential energy yield. This ensures the WtE system's output is realistically quantified and corresponds to the composition-specific calorific value.

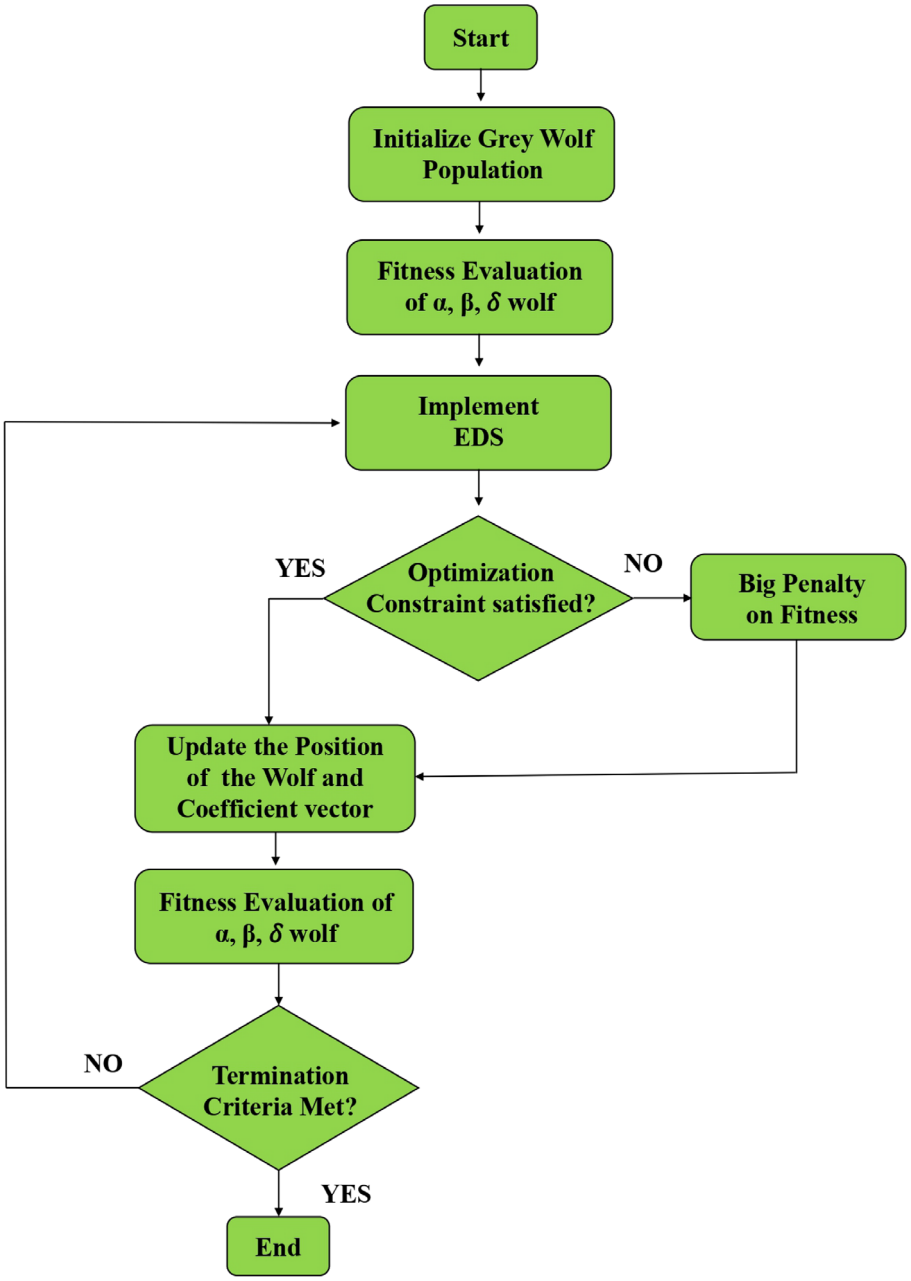

FIGURE 5 | GWO flowchart.

6.2 | Load Demand

A basic load consumption mode is designed that takes into account all of the hours in a year. The requirements of wards 11, 25, and 26 in the Halishahar region are prioritized in the process of calculating the demand for power in that area. Power Grid Company of Bangladesh (PGCB) is the source of this information on the demand for load in terms of electricity [65]. The information regarding the electrical load demand is gathered from the Halishahar 132/33 kV grid substation in North Patenga, which is managed by PGCB Ltd. The demand data from the year 2021 were selected owing to their full availability and validation by ensuring accuracy and reliability for the analysis. According to the results of the load calculation, it is determined that the annual energy demand of this region is approximately 107,150 MWh.

Both the hourly and annual demand for the load that is necessary for this region are shown in Figure 8. The hourly load demands fluctuate with time, as seen in Figure 8a. The difference is a result of people's different ways of living. By the seasonal shifts, electrical consumption varies, and the overall consequence of these changes is shown in Figure 8b.

6.3 | Renewable Resource

The location-specific resource data are collected from the NASA POWER [66] for the case study as shown in Figure 9. Figures 9, 9b, and Fig 9c represent annual hourly data of solar radiation, wind speed, and ambient temperature for the selected area, respectively.

FIGURE 6 | Location of the research area [63].

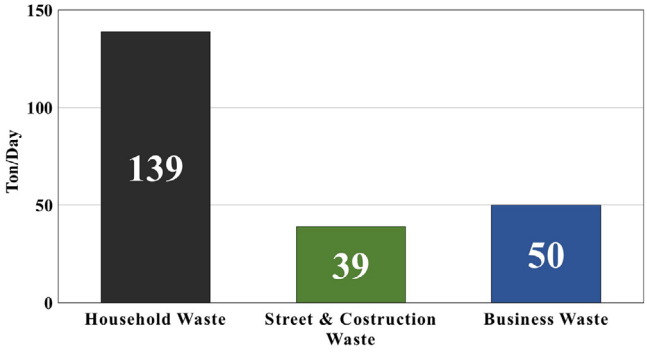

FIGURE 7 | Waste streams for selected site.

7 | Results and Discussions

Overall minimum number of sizing is required for the system to run economically feasible, microgrid's annual energy output, economic cost, and carbon emission are discussed in this section.

7.1 | Optimization Results

Both optimization methods had their maximum number of iterations set to 100 and their maximum number of search agents set to 500, with all other parameters and bounds of the optimized variables left unchanged. Optimal output is achieved by using the optimal combination of WtE, PV modules, WT, battery banks, and DG, hence the size of the microgrid system is responsible for LCoE, which is determined by these factors. The comparison between performance, mainly convergence rate of both optimization approaches, is depicted in Figure 10. In contrast to PSO, which requires numerous areas of convergence under the same constraint to reach a fitness value comparable to that of GWO, the convergence rate in GWO was substantially faster. After proceeding with less than 8 iterations, GWO was able to achieve the optimal sizing that has minimum LCoE for our system which is 0.221 $/kWh, while PSO took almost 80 iterations more to achieve 0.223 $/kWh. While searching on a specific space with a random integer value for size, the optimal fitness is evaluated from around 100 × 500 set. GWO outperformed PSO in managing the mix of linear and nonlinear components as well as the economic assessment model to provide the best possible result.

7.2 | Statistical Analysis

All parameter-based modifications are simulated to meet load requirements. In Figure 11, monthly sums of PSO and GWO output are shown. Both optimization techniques plot the power system's monthly electricity production and load demand. The total amount of energy produced by PV, wind, and WtE is determined using the method outlined in Section 2.

The assessment of annual energy usage output using two different optimization algorithms shows that there is some discrepancy in overall monthly power generation, even though the load demand stayed the same. This was mainly because the objective function was focused on choosing optimal annual cost, not counting other factor, because of that one assessment taken into consideration of diesel generator, which reliable and low cost generator which is reflected on minor discrepency in monthly generated output for respective assessment.

Overall, the results are quite similar, indicating that both algorithms effectively enhance the depiction of the yearly solar energy output generated by PV panels, as shown in Figure 12. Using the provided information, PSO performed an optimization and determined that this system is capable of producing 65,830 MWh of solar energy annually. According to the calculations done by GWO, this system has the potential to generate 71,888 MWh of solar energy every single year. The annual production of wind energy is depicted in Figure 13.

The figure illustrates the production of wind energy, which is represented by the color blue. Based on the available data, PSO has determined that the system in question has an annual wind energy output of 23,728 MWh. As per the projections furnished by GWO, this particular setup exhibits the capability to generate a total of 4724 MWh of wind power yearly. The graphical representation of the GWO output indicates that the production of wind energy is approximately twice that of the PSO output. During the midpoint of the year, the algorithms exhibit their maximum output generation.

Based on the available data, PSO has determined that the annual output of the system's WtE amounts to 51,766 MWh as shown in Figure 14. Based on GWO's projections, this particular system is anticipated to produce an annual output of 63,807 MWh of WtE. Both plots are depicted using the hue green. The production of WtE exhibits a slight increase in the geographic region of GWO when compared to that of PSO. The PSO diagram illustrates that the amount of WtE generation in winter is comparatively lower than that of GWO.

Solar energy has emerged as the undisputed victor in the race to become the optimal solution for satisfying the majority of electrical needs. Based on this chart, it looks like information about WtE energy production is closely related to information

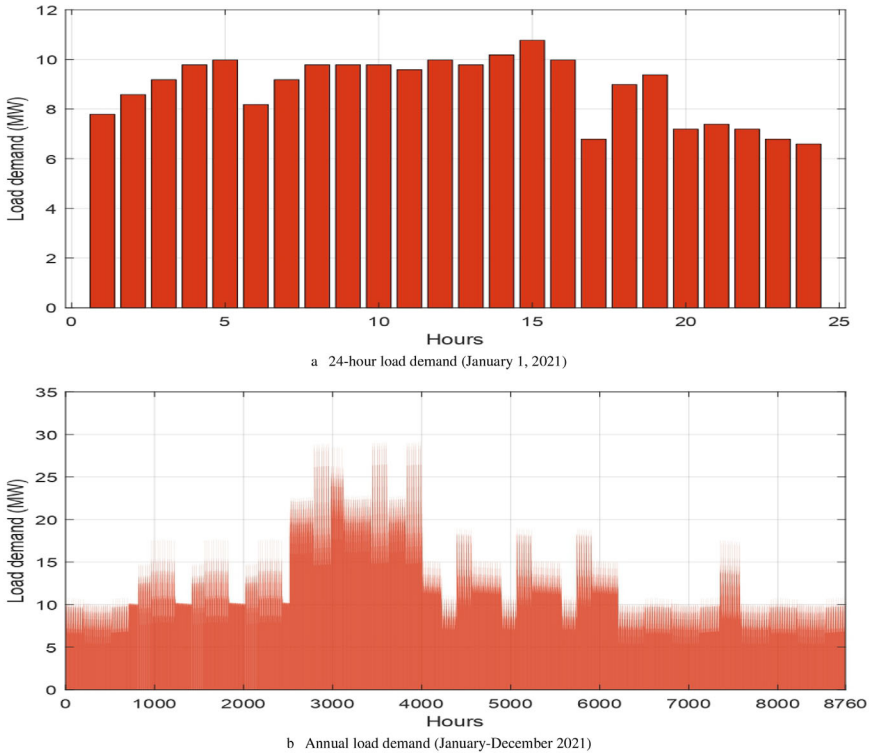

FIGURE 8 | Load demand of Halishahar

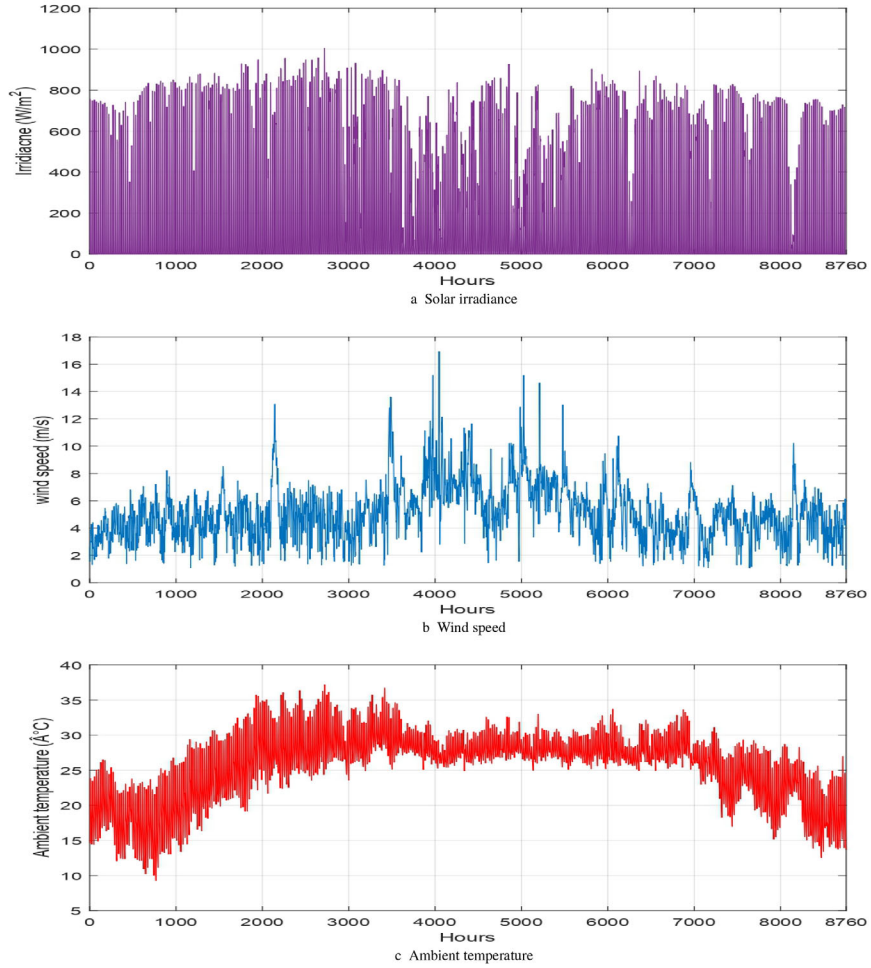

FIGURE 9 | Hourly renewable resource input data of Halishahar.

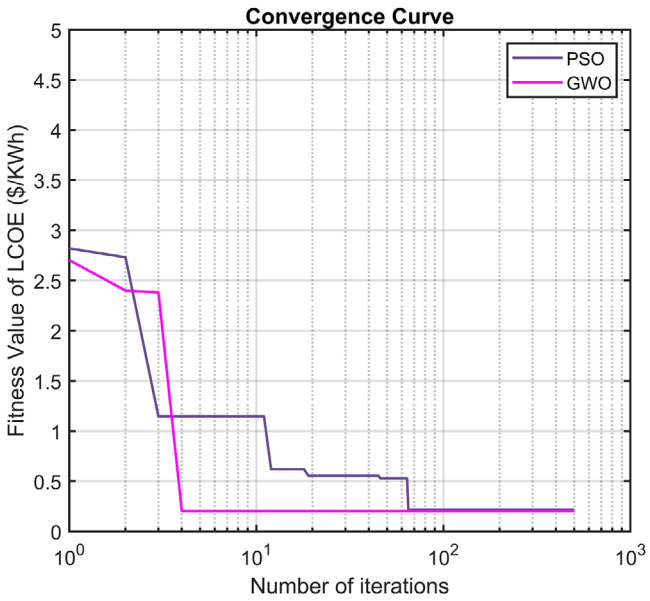

FIGURE 10 | Convergence curve of PSO and GWO.

about how much energy is used. The prediction that the output of WT will be at its lowest is made by both versions of the algorithm, and there is no substantial difference between them. Figure 15 displays a contrast between PSO and GWO algorithm results for meeting load demands while using RE sources. It is now abundantly clear that solar energy is the primary source of electricity for most of needs. At night, however, solar power generation is impossible as the sun is not available at that time.

The accumulated solar energy stored within the battery bank during daylight hours serves as a backup resource for nocturnal energy consumption. The WtE energy output appears to be closely associated with energy consumption rates. Both algorithm models predict the wind turbine's lowest output.

In contrast to the figure presented by PSO, it can be observed that GWO's amount of summer WtE generation is comparatively lower than that of PSO. In Figure 16, the results are compared for both algorithms when trying to meet the monthly load requirement with RE sources.

The annual CO_2 emission from the WtE and DG system is plotted in Figure 17. The hourly emitted CO_2 by the PSO and GWO optimized system is shown in Figures 17a and 17b, respectively. According to both optimization results, PSO, the optimized system, is producing around 27177-tonne equivalent CO_2 compared to the GWO-optimized system, which is around 33702-tonne equivalent CO_2. PSO performed better in minimizing the carbon footprint alongside the LCoE.

Annual energy generation from each microgrid component is shown in Figure 18 from the various optimization strategies.

The statistical results of PSO and GWO are summarized and compared in Table 5. The addition of WtE technology within the microgrid system offered a significant improvement in cost-effectiveness. The LCoE for the system configuration without WtE was determined to be 0.694 $/kWh using HOMER.

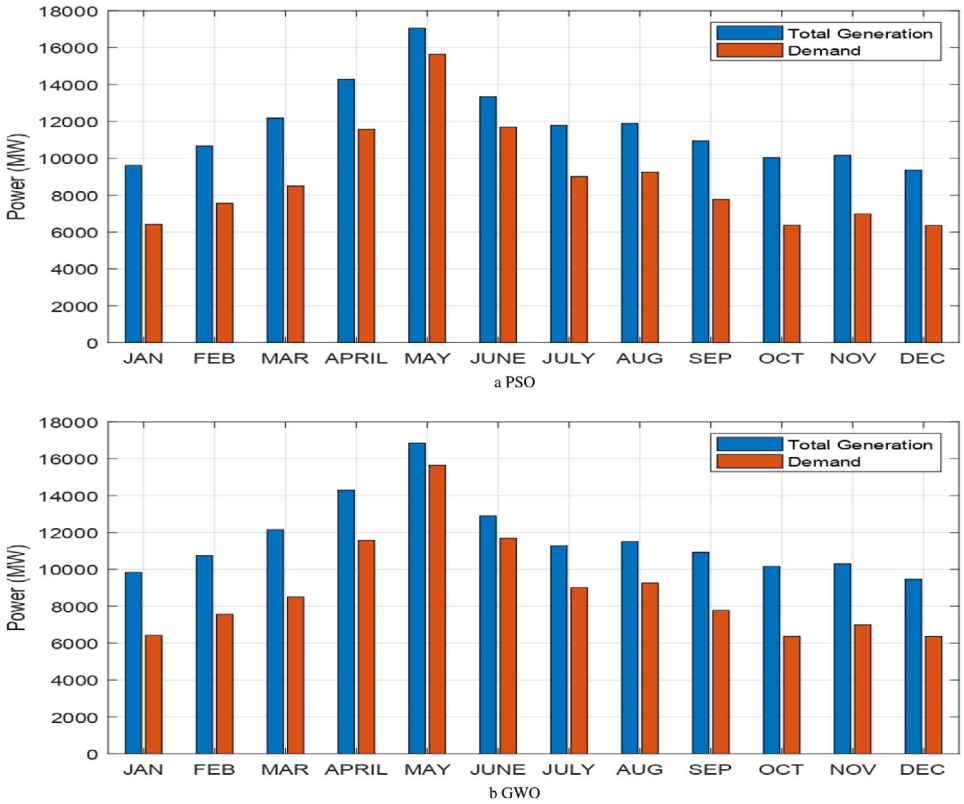

FIGURE 11 | Total generation vs load demand (monthly).

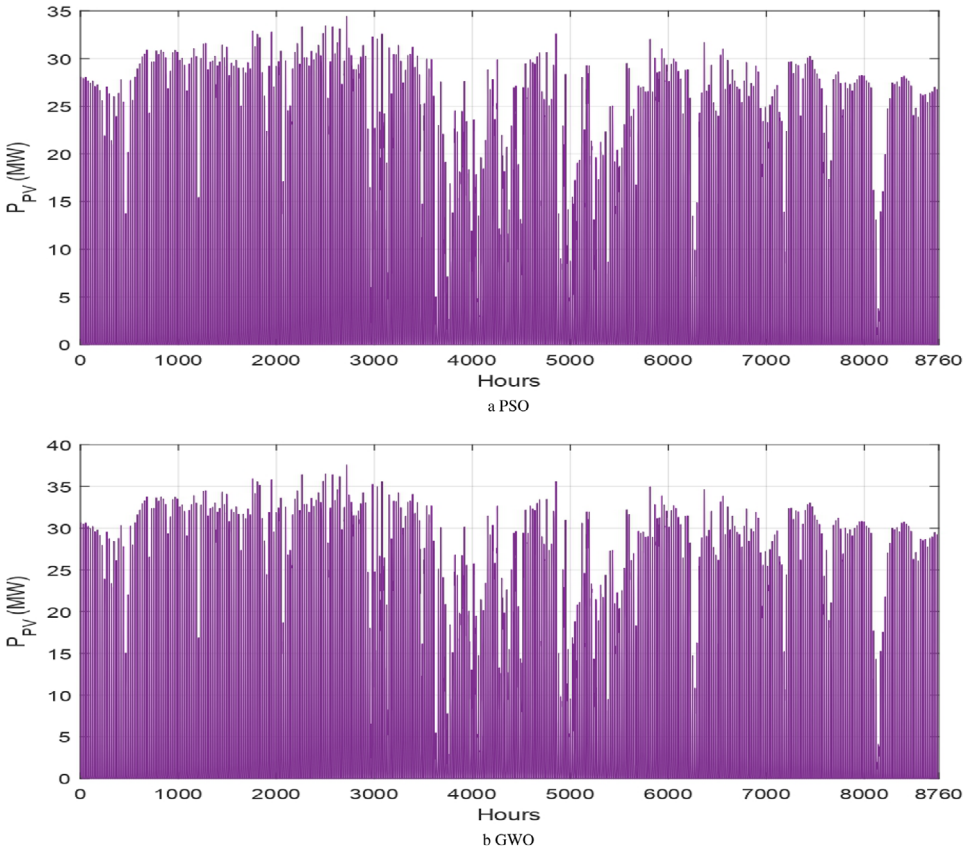

FIGURE 12 | PV generation.

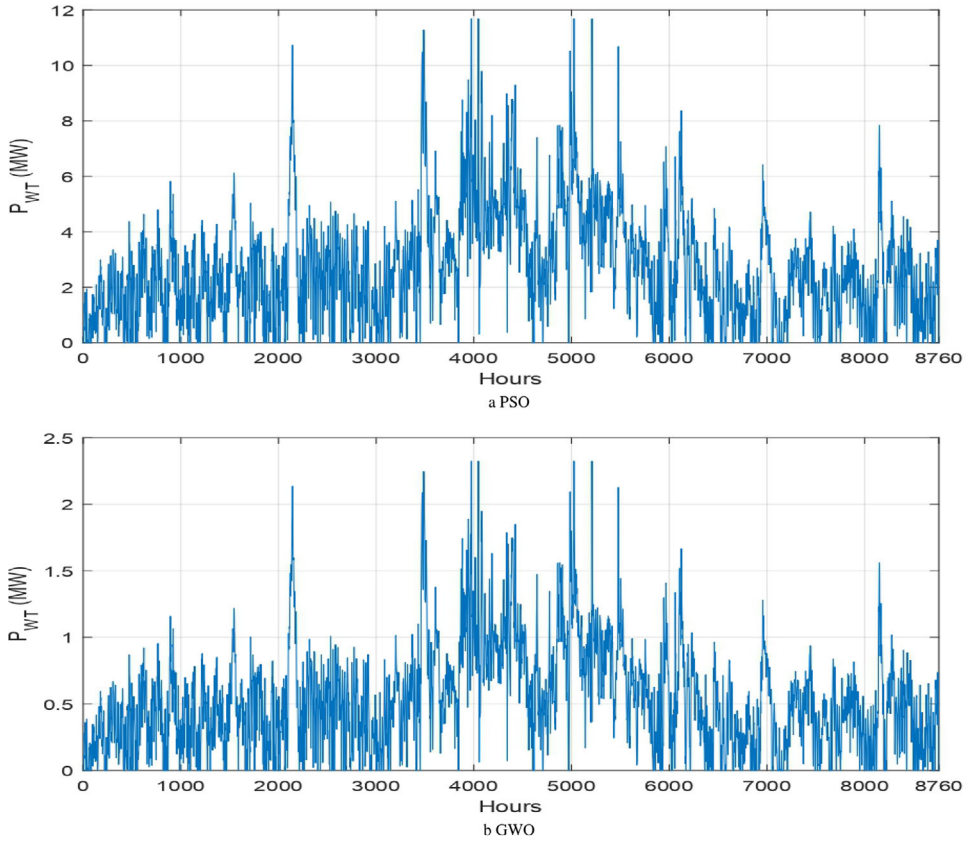

FIGURE 13 | WT generation.

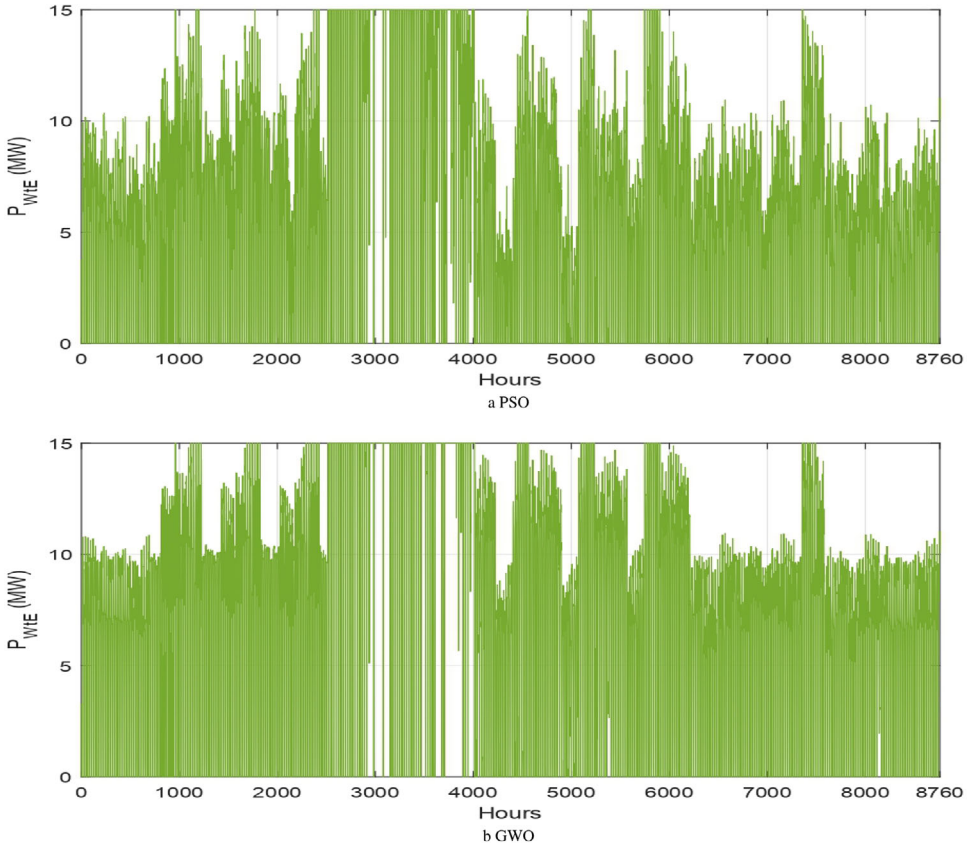

FIGURE 14 | WtE generation.

TABLE 5 | Microgrid optimized by algorithms.

Component name	Capacity (kW)		Net energy provided (MWh)		Annual cost ($)	
—	PSO	GWO	PSO	GWO	PSO	GWO
PV	39969	43648	65830	71888	92.41M	100.9M
WT	11679	2325	23728	4724	62.43M	12.43M
WtE	25000	25000	51766	63807	164.3M	188.5M
Battery	27903	31203	2871.9	4829.1	68.95M	77.11M
DG	0	1000	0	4.795	0	4.91M

It is noteworthy that the GWO includes a small diesel generator (DG) of 1000 kW capacity, which contributes only 4.795 MWh annually, while the PSO-based solution completely omits diesel usage. This slight inclusion in the GWO result is due to the algorithm's adaptive search behavior that attempts to ensure backup reliability in extreme scenarios of renewable shortfall, thereby slightly enhancing system feasibility at a minimal cost. The PSO configuration, while slightly higher in LCoE, avoids DG usage altogether, thus achieving a better emission profile. These differences underscore the variability of solution pathways among optimization algorithms while achieving similar overall performance.

In contrast, the LCoE for the system configuration with WtE was found to be 0.468 $/kWh. The integration of WtE technology resulted in a 22.6% reduction in LCoE for the system, indicating a favorable influence of WtE on the system's overall efficiency. The integration of WtE technology serves to broaden the range of energy sources while also promoting environmental sustainability through the utilization of waste resources. The present study highlights the significance of incorporating WtE in the optimization of microgrids to attain energy solutions that are both cost-effective and sustainable in remote and rural regions. For instance, a hybrid PV-biogas system reported LCOE of 0.187 $/kWh in liquids cryogenic energy storage system with a multi-objective optimization approach, whereas this study achieved a lower LCOE of 0.121 $/kWh using GWO, reflecting improved optimization performance [27]. Similarly, the total system cost for a comparable WtE setup was 12.5% higher than in this case, largely due to less efficient resource allocation [67]. In terms of CO_2 emissions, this proposed system showed a reduction of 8%–10% compared to the configurations analyzed in refer-

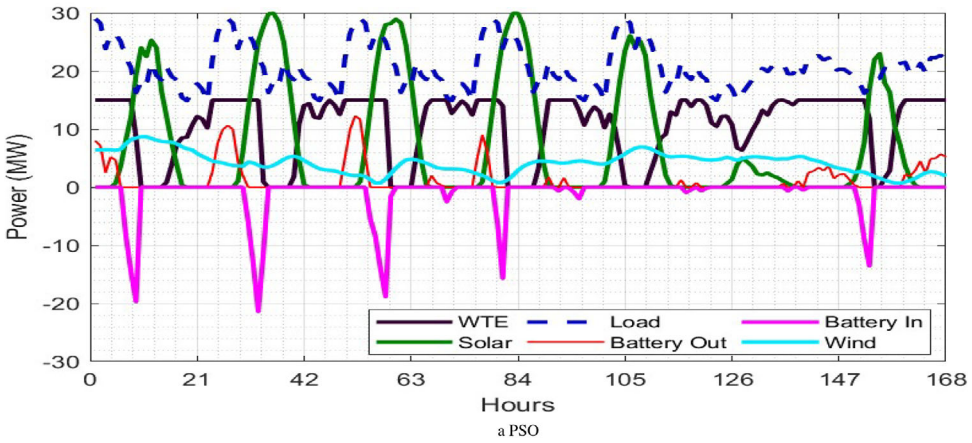

a PSO

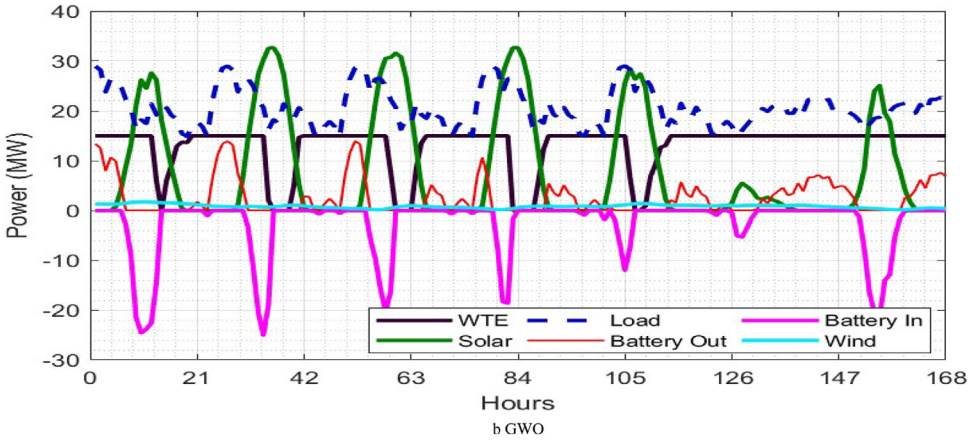

b GWO

FIGURE 15 | Renewable sources generation comparison (hourly).

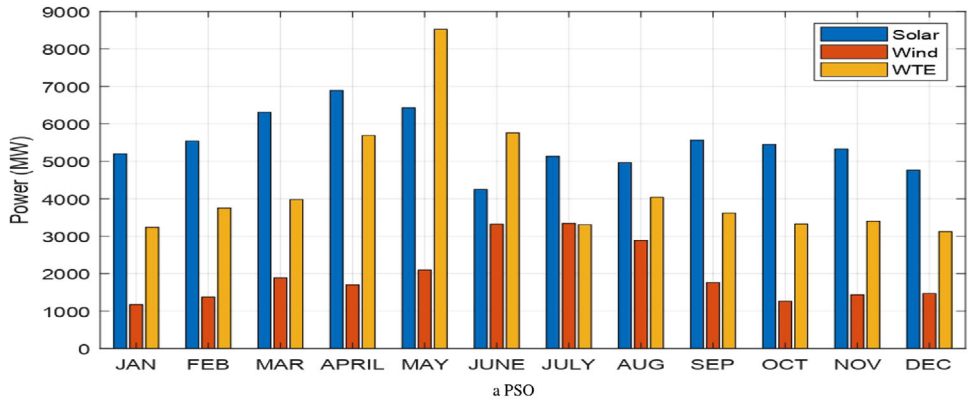

a PSO

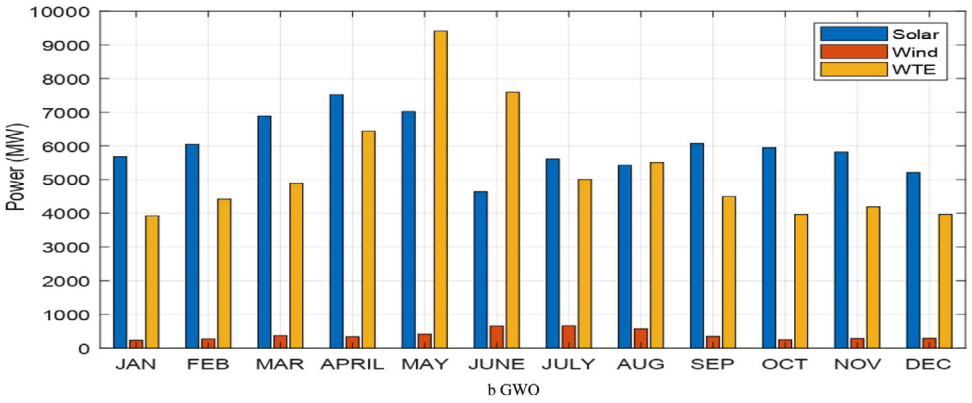

b GWO

FIGURE 16 | Renewable sources generation comparison (monthly).

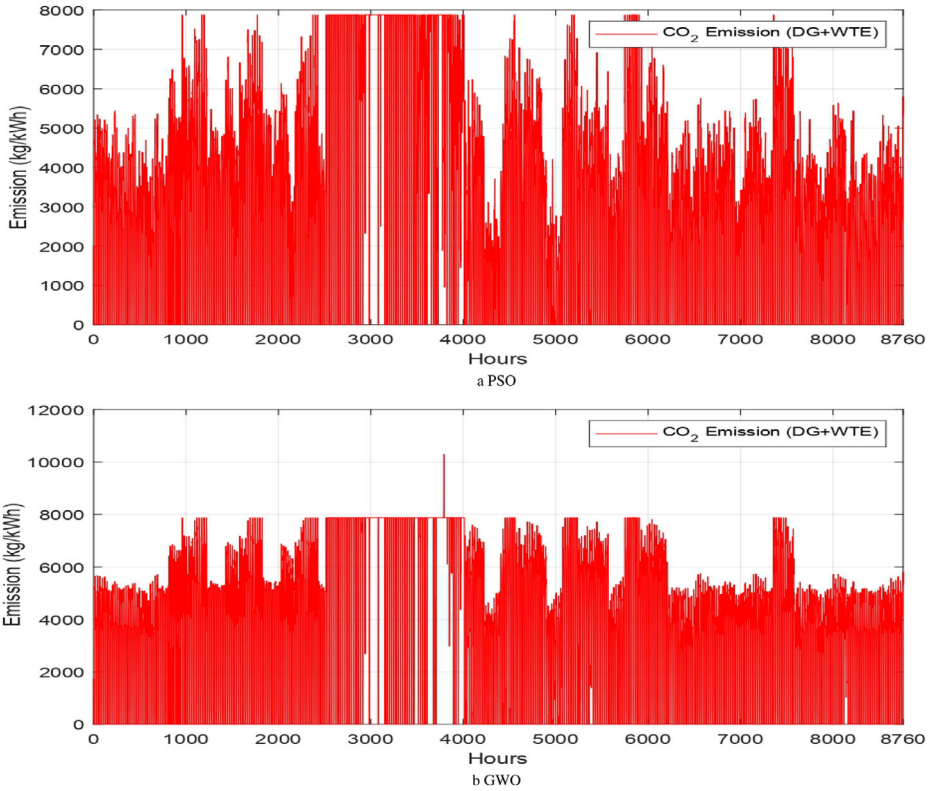

FIGURE 17 | CO_2 emission.

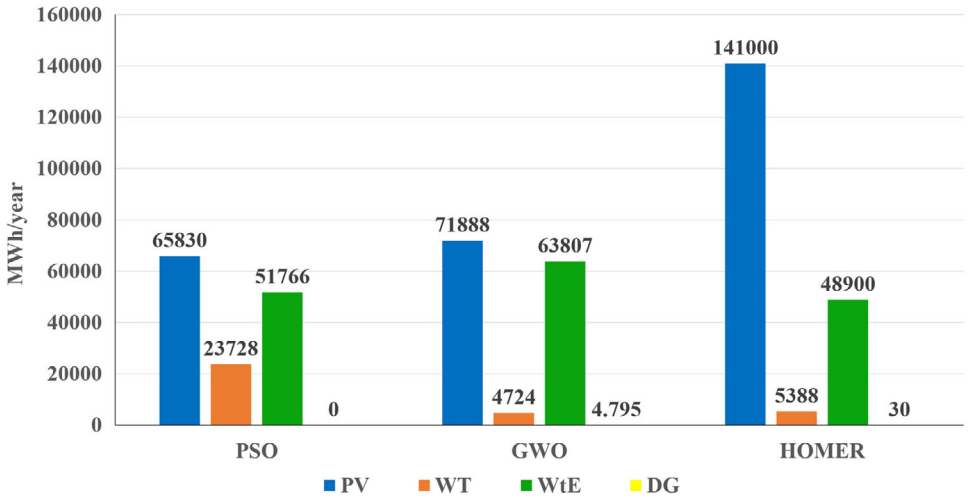

FIGURE 18 | Microgrid components annual generation for optimization methods.

ence [68], further confirming the environmental merit of this approach.

The varying LCoE values for each algorithm are a result of the distinct features of the system that make up each approach, presented in Table 6. The LCoE is the per kilowatt-hour of energy generation cost by the optimized proposed microgrid. The reduced LCoE suggests that the microgrid system is more deployable. GWO optimization achieves the lowest LCoE at 0.221 $/kWh. It suggests that the GWO-optimized system may satisfy the load requirement for the least expensive price. In addition, the statistical analysis showed that the utilized optimization methods

TABLE 6 | Overall comparison of algorithms.

Parameters	Optimization technique		
—	PSO	GWO	HOMER
Total generation (MWh/yr)	1,41,324	1,40,423.8	1,95,318.5
Dump energy (MWh)	30984	30512	88,168
CO_2 emission (t/yr)	27177	33502	35693
Annual cost ($)	388.1M	383.9M	719M
LCoE ($/kWh)	**0.223**	**0.221**	**0.468**

TABLE 7 | Comparative studies.

Ref.	Study region	Microgrid structure	Year	LCOE ($/kWh)
[69]	Pakistan	PV, WT and hydrogen storage	2024	$0.413
[70]	India	PV, WT, DG and BT	2024	$0.403
[71]	Sri Lanka	PV and battery energy	2024	$0.366
[72]	Saudi Arabia	PV, battery, thermal, and hydrogen storage	2024	$0.252
[73]	West Africa	PV, battery and biomass	2025	$0.202

had an acceptable level of performance stability, with the GWO algorithm being preferable.

7.3 | CO_2 Emission Reduction Estimation

It is determined that the annual CO_2 emission is less than the standard practice. In comparison to more traditional methods of power generation, both of these optimization techniques result in a significant reduction of CO_2 emissions. There is just one component in the microgrid that is optimized using PSO that produces carbon dioxide, and that is the WtE. However, the GWO-optimized microgrid consists of two components, namely WtE and DG, both of which are responsible for the emission of CO_2. Therefore, the microgrid that is optimized using PSO releases less CO_2 into the atmosphere than the microgrid using GWO.

7.4 | Comparative Study

A comparative analysis of similar studies among some regional country is provided in Table 7, as the different approach integration model are reported with their LCoE.

Although some studies in Table 7 report lower absolute LCoE values, such direct comparisons must be interpreted with caution. Differences in renewable resource quality, technology composition, capital/operational cost assumptions, and reliability requirements strongly influence reported outcomes. In this study, the effectiveness of the proposed method is defined relative to controlled baselines under the same constraints. Specifically, integrating WtE reduces HOMER's LCoE from 0.694 to 0.468 $/kWh (−22.6%), and further optimization with GWO lowers LCoE to 0.221 $/kWh (−52.8% vs. HOMER with WtE), while meeting the full annual demand of 107,150 MWh. By contrast, lower values reported elsewhere often omit WtE costs or assume different regional resource profiles, limiting direct comparability.

8 | Conclusions

This study proposed an optimized hybrid microgrid that incorporates renewable energy and WtE systems to reduce the LCoE and emissions. By applying PSO and GWO algorithms, we identified the most cost-effective configurations for the Halishahar region in Bangladesh. Results show that integrating WtE significantly improves economic and environmental performance, achieving a 22.6% LCoE reduction compared to configurations without WtE. The GWO-based design yielded the lowest LCoE ($0.221/kWh), while PSO resulted in lower CO_2 emissions. These findings underscore the potential of WtE-integrated microgrids in advancing sustainable, decentralized energy systems in developing regions. This work provides a replicable framework for future optimization-based microgrid planning, especially in contexts with high municipal waste availability and limited grid access.

Future studies should focus on applying this method to assess system performance and response in scenarios involving grid integration, super-capacitors, and fuel cells, considering diverse geographic location data, renewable intermittency, and load demand inconsistency. This is crucial due to increasing energy demand from global development and the diminishing availability of energy resources, along with the imposition of additional limits that restrict the range of possible microgrid combinations that are accountable for reducing the LCoE. Despite this, both optimizations provide similar LCoE with varied size combinations of differing RES. This discrepancy can be mitigated by incorporating additional constraints into the objective function for future studies.

Author Contributions

Md. Sajjad – Ul Islam: conceptualization, data curation, formal analysis, funding acquisition, methodology, resources, software, visualization, writing – original draft, writing – review and editing. **Md. Arafat Bin Zafar:** conceptualization, data curation, formal analysis, investigation, methodology, resources, software, validation, visualization, writing – original draft. **Md. Rashidul Islam:** conceptualization, data curation, investigation, methodology, project administration, resources, supervision, validation, writing – review and editing. **Arafat Ibne Ikram:** formal analysis, methodology, resources, software, visualization, writing – original draft, writing – review and editing. **Md Shafiullah:** funding acquisition, investigation, supervision, validation, visualization, writing – review and editing.

Acknowledgements

The authors would like to acknowledge the research support provided by their affiliated institutions. Dr. Md Shafiullah would like to acknowledge the reserach support provided by the Deanship of Research at King Fahd University of Petroleum & Minerals, Dhahran, Saudi Arabia, under the Grant No. EC241001.

Conflicts of Interest

The authors declare no conflicts of interest.

Data Availability Statement

The data supporting the findings of this study are actually available from the corresponding author upon a reasonable request.

References

1. A. I. Osman, L. Chen, M. Yang, et al., "Cost, Environmental Impact, and Resilience of Renewable Energy Under a Changing Climate: A Review," *Environmental Chemistry Letters* 21, no. 2 (2023): 741–764.

2. S. M. Alshareef and A. Fathy, "Efficient red Kite Optimization Algorithm for Integrating the Renewable Sources and Electric Vehicle Fast Charging Stations in Radial Distribution Networks," *Mathematics* 11, no. 15 (2023): 3305.

3. S. M. Rahman, F. S. M. Al-Ismail, M. E. Haque, et al., "Electricity Generation in Saudi Arabia: Tracing Opportunities and Challenges to Reducing Greenhouse gas Emissions," *IEEE Access* 9 (2021): 116 163–116 182.

4. F. Dehghani and M. A. Shafiyi, *IET Renewable Power Generation* 17, no. 15 (2023): 3638–3650.

5. A. I. Ikram, S. E. A. Himu, T. Khandaker, et al., "Design Optimization and Assessment of Floating Solar pv With Wind Turbine Systems at Kepz," in *2023 5th International Conference on Sustainable Technologies for Industry 5.0 (STI)* (IEEE, 2023), 1–6.

6. A. I. Ikram, M. S.-U. Islam, M. A. B. Zafar, M. K. Rocky, Imtiaz, and A. Rahman, "Techno-Economic Optimization of Grid-Integrated Hybrid Storage System Using Genetic Algorithm," in *2023 1st International Conference on Innovations in High Speed Communication and Signal Processing (IHCSP)* (IEEE, 2023), 300–305.

7. M. Shafiullah, S. D. Ahmed, and F. A. Al-Sulaiman, "Grid Integration Challenges and Solution Strategies for Solar pv Systems: A Review," *IEEE Access* (2022).

8. C. A. Nallolla, V. P, D. Chittathuru, and S. Padmanaban, "Multi-Objective Optimization Algorithms for a Hybrid ac/dc Microgrid Using Res: A Comprehensive Review," *Electronics* 12, no. 4 (2023): 1062.

9. A. Kumar, S. Sharma, and A. Verma, "Optimal Sizing and Multi-Energy Management Strategy for pv-Biofuel-Based off-Grid Systems," *IET Smart Grid* 3, no. 1 (2020): 83–97.

10. S. Ahmad, M. Shafiullah, C. B. Ahmed, and M. Alowaifeer, "A review of microgrid energy management and control strategies," *IEEE Access* 11 (2023): 21729–21757.

11. M. R. Pranta, M. S. Alam, S. E. A. Himu, et al., "Small Scale pv Integration in Bangladesh: Opportunities, Challenges, and Recommendation," in *2023 10th IEEE International Conference on Power Systems (ICPS)* (IEEE, 2023), 1–6, https://doi.org/10.1109/ICPS60393.2023.10428825.

12. D. Yang, C. Jiang, G. Cai, and N. Huang, "Optimal Sizing of a Wind/Solar/Battery/Diesel Hybrid Microgrid Based on Typical Scenarios Considering Meteorological Variability," *IET Renewable Power Generation* 13, no. 9 (2019): 1446–1455.

13. M. Shafiey Dehaj and H. Hajabdollahi, "Multi-Objective Optimization of Hybrid Solar/Wind/Diesel/Battery System for Different Climates of Iran," *Environment, Development and Sustainability* 23, no. 7 (2021): 10910–10936.

14. Y. Pavankumar, R. Kollu, and S. Debnath, "Multi-Objective Optimization of Photovoltaic/Wind/Biomass/Battery-Based Grid-Integrated Hybrid Renewable Energy System," *IET Renewable Power Generation* 15, no. 7 (2021): 1528–1541.

15. U. B. Tayab, F. Yang, M. El-Hendawi, and J. Lu, "Energy Management System for a Grid-Connected Microgrid With Photovoltaic And Battery Energy Storage System," in *2018 Australian & New Zealand Control Conference (ANZCC)* (IEEE, 2018), 141–144.

16. A. I. Ikram, A. Ullah, D. Datta, A. Islam, and T. Ahmed, "Optimizing Energy Consumption in Smart Homes: Load Scheduling Approaches," *IET Power Electronics* 17, no. 16 (2024): 2656–2668.

17. K. S. EI-Bidairi, H. D. Nguyen, S. Jayasinghe, and T. S. Mahmoud, "Multiobjective Intelligent Energy Management Optimization for Grid-Connected Microgrids," in *2018 IEEE International Conference on Environment and Electrical Engineering and 2018 IEEE Industrial and Commercial Power Systems Europe (EEEIC/I&CPS Europe)* (IEEE, 2018), 1–6.

18. K. Basaran, N. S. Cetin, and S. Borekci, "Energy Management for on-Grid and off-Grid Wind/pv and Battery Hybrid Systems," *IET Renewable Power Generation* 11, no. 5 (2017): 642–649.

19. B. Dey, F. P. G. Márquez, P. K. Panigrahi, and B. Bhattacharyya, "A Novel Metaheuristic Approach to Scale the Economic Impact of Grid Participation on a Microgrid System," *Sustainable Energy Technologies and Assessments* 53 (2022): 102417.

20. P. Ziyaei, M. Khorasanchi, H. Sayyaadi, and A. Sadollah, "Minimizing the Levelized Cost of Energy in an Offshore Wind Farm With non-Homogeneous Turbines Through Layout Optimization," *Ocean Engineering* 249 (2022): 110859.

21. P. Sun, T. Yun, and Z. Chen, "Multi-Objective Robust Optimization of Multi-Energy Microgrid With Waste Treatment," *Renewable Energy* 178 (2021): 1198–1210.

22. S. Mohseni, A. C. Brent, and D. Burmester, "A Comparison of Metaheuristics for the Optimal Capacity Planning of an Isolated, Battery-Less, Hydrogen-Based Micro-Grid," *Applied Energy* 259 (2020): 114224.

23. A. I. Ikram, M. Shafiullah, M. R. Islam, and M. K. Rocky, "Techno-Economic Assessment and Environmental Impact Analysis of Hybrid Storage System Integrated Microgrid," *Arabian Journal for Science and Engineering* 49, no. 12 (Dec 2024): 15 917–15 934.

24. F. S. Islam, "Artificial Intelligence-Driven Optimization and Decision Support for Integrated Waste-to-Energy Systems in Climate-Vulnerable Megacities: A Case Study of Dhaka, Bangladesh," *International Journal of Applied and Natural Sciences* 3, no. 2 (2025): 01–34.

25. M. A. B. Zafar, M. R. Islam, M. S.-U. Islam, M. Shafiullah, and A. I. Ikram, "Economic Analysis and Optimal Design of Micro-Grid Using Pso Algorithm," in *2022 12th International Conference on Electrical and Computer Engineering (ICECE)* (IEEE, 2022), 421–424.

26. G. N. Oliveira, T. Costa, M. A. Mohamed, A. Ilinca, and M. H. Marinho, "Comprehensive Case Study on the Technical Feasibility of Green Hydrogen Production From Photovoltaic and Battery Energy Storage Systems," *Energy Science & Engineering* 12, no. 10 (2024): 4549–4565.

27. Z. Liu, J. Shao, H. Guan, et al., "Optimization of a Novel Liquid Carbon Dioxide Energy Storage System by Thermodynamic Analysis and Use of Solar Energy and Liquefied Natural gas," *Applied Thermal Engineering* 258 (2025): 124555.

28. H. Chen, S. Yang, H. Wu, J. Song, and S. Shui, "Advanced Hierarchical Energy Optimization Strategy for Integrated Electricity-Heat-Ammonia Microgrid Clusters in Distribution Network," *International Journal of Hydrogen Energy* 97 (2025): 1481–1497.

29. P. García-Gutiérrez, A. M. Amadei, D. Klenert, et al., "Environmental and Economic Assessment of Plastic Waste Recycling and Energy Recovery Pathways in the eu," *Resources, Conservation and Recycling* 215 (2025): 108099.

30. M. Xu, J. Zhang, Z. Wen, P. Wang, and J. Chen, "Economic and Environmental Assessment of Plant-Level Decarbonization in Waste-to-Energy Industry With Ccus Technology: Evidence From China," *Applied Energy* 381 (2025): 125148.

31. Z. Guo, W. Wei, M. Shahidehpour, Z. Wang, and S. Mei, "Optimisation Methods for Dispatch and Control of Energy Storage With Renewable Integration," *IET Smart Grid* 5, no. 3 (2022): 137–160.

32. X. Qiao, J. Ding, C. She, W. Mao, A. Zhang, B. Feng, and Y. Xu, "A Metaheuristic Multi-Objective Optimization of Energy and Environmental Performances of a Waste-to-Energy System Based on Waste Gasification Using Particle Swarm Optimization," *Energy Conversion and Management* 317 (2024): 118844.

33. A. L. Bukar, C. W. Tan, and K. Y. Lau, "Optimal Sizing of an Autonomous Photovoltaic/Wind/Battery/Diesel Generator Microgrid Using Grasshopper Optimization Algorithm," *Solar Energy* 188 (2019): 685–696.

34. B. K. Das, R. Hassan, M. S. H. Tushar, F. Zaman, M. Hasan, and P. Das, "Techno-Economic and Environmental Assessment of a Hybrid

Renewable Energy System Using Multi-Objective Genetic Algorithm: A Case Study for Remote Island in Bangladesh," *Energy Conversion and Management* 230 (2021): 113823.

35. N. Alshammari and J. Asumadu, "Optimum Unit Sizing of Hybrid Renewable Energy System Utilizing Harmony Search, Jaya and Particle Swarm Optimization Algorithms," *Sustainable Cities and Society* 60 (2020): 102255.

36. M. A. B. Zafar, M. S.-U. Islam, M. R. Islam, and M. Shafiullah, "Optimized Waste to Energy Technology Combined With PV-Wind-Diesel for Halishahar in Chattogram," in *2022 IEEE International Conference on Electronics, Computing and Communication Technologies (CONECCT)* (IEEE, 2022), 1–5.

37. "Complete Fastox System & Plant," accessed July 20, 2022, https://sierraenergy.com/complete-fastox-system-plant/.

38. R. Ibikunle, I. Titiladunayo, B. Akinnuli, A. Lukman, P. Ikubanni, and O. Agboola, "Modelling the Energy Content of Municipal Solid Waste and Determination of its Physico-Chemical Correlation Using Multiple Regression Analysis," *International Journal of Mechanical Engineering and Technology* 9, no. 11 (2018): 220–232, https://eprints.lmu.edu.ng/1696/.

39. R. Ibikunle, I. Titiladunayo, B. Akinnuli, S. Dahunsi, and T. Olayanju, "Estimation of Power Generation From Municipal Solid Wastes: A Case Study of Ilorin Metropolis, Nigeria," *Energy Reports* 5 (2019): 126–135.

40. M. A. Ramli, H. Bouchekara, and A. S. Alghamdi, "Optimal Sizing of pv/Wind/Diesel Hybrid Microgrid System Using Multi-Objective Self-Adaptive Differential Evolution Algorithm," *Renewable Energy* 121 (2018): 400–411.

41. N. Yimen, T. Tchotang, A. Kanmogne, et al., "Optimal Sizing and Techno-Economic Analysis of Hybrid Renewable Energy Systems–a Case Study of a Photovoltaic/Wind/Battery/Diesel System in Fanisau, Northern Nigeria," *Processes* 8, no. 11 (2020): 1381.

42. S. Dhundhara, Y. P. Verma, and A. Williams, "Techno-Economic Analysis of the Lithium-Ion and Lead-Acid Battery in Microgrid Systems," *Energy Conversion and Management* 177 (2018): 122–142.

43. M. M. Samy, M. I. Mosaad, M. F. El-Naggar, and S. Barakat, "Reliability Support of Undependable Grid Using Green Energy Systems Economic Study," *IEEE Access* 9 (2021): 14 528–14 539.

44. Y. Wang and Y. Yang, "Research on Greenhouse gas Emissions and Economic Assessment of Biomass Gasification Power Generation Technology in China Based on LCA Method," *Sustainability* 14, no. 24 (2022): 16729.

45. F. M. de Melo, A. Silvestre, and M. Carvalho, "Carbon Footprints Associated With Electricity Generation From Biomass Syngas and Diesel," *Environmental Engineering & Management Journal (EEMJ)* 18, no. 7 (2019).

46. A. Lorestani and M. Ardehali, "Optimal Integration of Renewable Energy Sources for Autonomous tri-Generation Combined Cooling, Heating and Power System Based on Evolutionary Particle Swarm Optimization Algorithm," *Energy* 145 (2018): 839–855.

47. S. S. Singh and E. Fernandez, "Modeling, Size Optimization and Sensitivity Analysis of a Remote Hybrid Renewable Energy System," *Energy* 143 (2018): 719–731.

48. W. Shen, X. Chen, J. Qiu, et al., "A Comprehensive Review of Variable Renewable Energy Levelized Cost of Electricity," *Renewable and Sustainable Energy Reviews* 133 (2020): 110301.

49. M. D. Qandil, R. S. Amano, and A. I. Abbas, "A Stand-Alone Hybrid Photovoltaic, Fuel Cell and Battery System," in *Energy Sustainability*, Vol. 51418 (American Society of Mechanical Engineers, 2018), V001T12A001.

50. "Waste-to-Energy: One Solution for two Problems," accessed July 28, 2022, https://www.energyforgrowth.org/memo/.

51. S. Manmadharao, S. Chaitanya, B. V. rao, and G. Srinivasarao, "Design and Optimization of Grid Integrated Solar Energy System Using Homer Grid Software," in *2019 Innovations in Power and Advanced Computing Technologies (i-PACT)*, vol. 1 (IEEE, 2019), 1–5.

52. M. Papadimitrakis, N. Giamarelos, M. Stogiannos, E. Zois, N.-I. Livanos, and A. Alexandridis, "Metaheuristic Search in Smart Grid: A Review With Emphasis on Planning, Scheduling and Power Flow Optimization Applications," *Renewable and Sustainable Energy Reviews* 145 (2021): 111072.

53. H. Rezaei, O. Bozorg-Haddad, and X. Chu, "Grey Wolf Optimization (gwo) Algorithm," in *Advanced Optimization by Nature-Inspired Algorithms* (Springer, 2018), 81–91.

54. "How Homer Optimization Works," accessed January 10, 2024, https://www.homerenergy.com/products/grid/docs/1.1/index.html.

55. H. Elaouni, H. Obeid, S. Le Masson, O. Foucault, and H. Gualous, "A Comparative Study for Optimal Sizing of a Grid-Connected Hybrid System Using Genetic Algorithm, Particle Swarm Optimization, and HOMER," in *IECON 2021–47th Annual Conference of the IEEE Industrial Electronics Society* (IEEE, 2021), 1–6.

56. M. Camas-Náfate, A. Coronado-Mendoza, C. Vargas-Salgado, J. Águila-León, and D. Alfonso-Solar, "Optimizing Lithium-ion Battery Modeling: A Comparative Analysis of pso and gwo Algorithms," *Energies* 17, no. 4 (2024): 822.

57. T.-H. Kim and J.-I. Byun, "Truss Sizing Optimization With a Diversity-Enhanced Cyclic Neighborhood Network Topology Particle Swarm Optimizer," *Mathematics* 8, no. 7 (2020): 1087.

58. Z.-M. Liu, X.-G. Gao, Y. Pan, and B. Jiang, "Multi-Objective Parameter Optimization of Submersible Well Pumps Based on rbf Neural Network and Particle Swarm Optimization," *Applied Sciences* 13, no. 15 (2023): 8772.

59. S.-K. S. Fan and C.-H. Jen, "An Enhanced Partial Search to Particle Swarm Optimization for Unconstrained Optimization," *Mathematics* 7, no. 4 (2019): 357.

60. I. Ullah, K. Liu, T. Yamamoto, M. Shafiullah, and A. Jamal, "Grey Wolf Optimizer-Based Machine Learning Algorithm to Predict Electric Vehicle Charging Duration Time," *Transportation Letters* 15, no. 8 (2022): 889–906.

61. Z. Yue, S. Zhang, and W. Xiao, "A Novel Hybrid Algorithm Based on Grey Wolf Optimizer and Fireworks Algorithm," *Sensors* 20, no. 7 (2020): 2147.

62. H. Faris, I. Aljarah, M. A. Al-Betar, and S. Mirjalili, "Grey Wolf Optimizer: A Review of Recent Variants and Applications," *Neural Computing and Applications* 30 (2018): 413–435.

63. "Halishahar Thana," accessed June 12, 2022, https://en.banglapedia.org/index.php/Halishahar_Thana.

64. "Chattogram City Corporation," accessed July 18, 2022, https://ccc.portal.gov.bd/site/page/bb4d611d-880b-4ebc-958a-c00cc3ed20e7/-.

65. Power Grid Company of Bangladesh Ltd., accessed April 20, 2021, http://www.pgcb.gov.bd/.

66. "NASA POWER | Data Access Viewer, Prediction Of Worldwide Energy Resource," accessed July 15, 2022, https://power.larc.nasa.gov/data-access-viewer/.

67. M. Asim, R. Kumar, A. Kanwal, A. Shahzad, A. Ahmad, and M. Farooq, "Techno-Economic Assessment of Energy and Environmental Impact of Waste-to-Energy Electricity Generation," *Energy Reports* 10 (2023): 3373–3382.

68. P. H. Kumar, R. R. Gopi, R. Rajarajan, N. Vaishali, K. Vasavi, and S. Kumar, "Prefeasibility Techno-Economic Analysis of Hybrid Renewable Energy System," *e-Prime-Advances in Electrical Engineering, Electronics and Energy* 7 (2024): 100443.

69. H. M. El Zoghby, A. F. Bendary, and R. S. Afia, "Techno-Economic Study of a 100% Renewable Energy-Based Isolated Microgrid Involving Green Hydrogen Production," *Sustainable Energy Technologies and Assessments* 76 (2025): 104303.

70. A. Naseem, I. Ashraf, and M. M. Kamal, "Designing and Optimisation of Microgrid With Green Energy Source for Efficient Power Supply," in *International Conference on ICT for Digital, Smart, and Sustainable Development* (Springer, 2024), 57–71.

71. S. Forrousso, S. I. Kaitouni, A. Mana, et al., "Optimal Sizing of off-Grid Microgrid Building-Integrated-Photovoltaic System With Battery for a net Zero Energy Residential Building in Different Climates of Morocco," *Results in Engineering* 22 (2024): 102288.

72. A. Alemam, A. S. Al-Sumaiti, and I. Afgan, "Optimized Hybrid Storage Standalone Microgrid With Electrical, Heat, and Hydrogen Loads Based on Stochastic Photovoltaic Modelling," *Energy Conversion and Management: X* 27 (2025): 101091.

73. I. Amoussou, M. R. Aza-Gnandji, M. Kplé, et al., "Optimizing an Autonomous Microgrid Based on Renewable Energy Systems for Rural Electrification in Benin," SSRN 5101048.

Appendix A

In PSO technique, particles or each solutions represent system configurations (number of component needed for the system to run optimally), updating their velocities and positions based on personal and global best.

ALGORITHM 1 | Iterative Steps for PSO.

Load Microgrid parameter (Meteorological data & Load demand data)

Initialize a population of N particles with random positions and velocities

Evaluate fitness of each particle using the objective function

Set each particle's personal best ($pbest$) and identify global best ($gbest$)

for $t = 1$ to MaxIterations **do**

for each particle i **do**

Update velocity:

$$v_i^{t+1} = wv_i^t + c_1 r_1 (pbest_i - x_i^t) + c_2 r_2 (gbest - x_i^t)$$

Update position:

$$x_i^{t+1} = x_i^t + v_i^{t+1}$$

Evaluate fitness for **cost function** of updated position

Update $pbest_i$ if new fitness is better

end for

Update $gbest$ among all particles

Penalty function:

if $Annual\ Energy\ Output < Annual\ Load\ Demand$ **then**

$$Fitness(t) = gbest \times Penalty$$

else

$$Fitness(t) = gbest$$

end if

end for

return best solution $gbest$

Appendix B

In GWO technique, three best candidate solutions (α, β, γ) are used to guide the remaining population towards the global optimum.

ALGORITHM 2 | Iterative Steps for GWO.

Load Microgrid parameter (Meteorological data & Load demand data)

Initialize a population of N wolves with random positions

Evaluate fitness of each wolf using the objective function

Identify α (best), β (second best), and γ (third best)

for $t = 1$ to MaxIterations **do**

for each wolf i **do**

Update coefficient vectors A and C

Compute distances from leaders:

$$D_\alpha = |C_1 \cdot X_\alpha - X_i|, \quad D_\beta = |C_2 \cdot X_\beta - X_i|, \quad D_\gamma = |C_3 \cdot X_\gamma - X_i|$$

Update positions based on leaders:

$$X_1 = X_\alpha - A_1 \cdot D_\alpha, \quad X_2 = X_\beta - A_2 \cdot D_\beta, \quad X_3 = X_\gamma - A_3 \cdot D_\gamma$$

$$X_i^{t+1} = \frac{X_1 + X_2 + X_3}{3}$$

end for

Penalty function:

if $Annual\ Energy\ Output < Annual\ Load\ Demand$ **then**

$$Fitness(t) = \alpha \times Penalty$$

else

$$Fitness(t) = \alpha$$

end if

end for

Recalculate fitness for **cost function** and update α, β, γ

return best solution α